12-2007

Spin Density Wave Phases in Semiconductor Superlattice

Liqiu Zheng
Clemson University, lzheng@clemson.edu

Spin Density Wave Phases in Semiconductor Superlattices

A Dissertation
Presented to
the Graduate School of
Clemson University

In Partial Fulfillment
of the Requirements for the Degree
Doctor of Philosophy
Theoretical Physics

---

by
Liqiu Zheng
December 2007

Accepted by:
Dr. Catalina Marinescu, Committee Chair
Dr. Joseph R. Manson
Dr. Pu-Chun Ke
Dr. Chad Sosolik

Abstract

We discuss the existence of spin instabilities and of possible ground states with broken spin symmetry in the presence of a tilted magnetic field for several semiconductor heterostructures. In each instance, the fundamental premise of our study is the existence of a spin degeneracy, controlled by tuning various experimentally controllable parameters, that permits the apparition of spin-flip processes driven entirely by the many-body Coulomb interaction. If in the case of a single quantum well, the spin instabilities trigger an abrupt paramagnetic to ferromagnetic phase transition, we demonstrate that in superlattices, at low temperatures, a stable spin density wave (SDW) ground state is supported for certain system parameters that allow a substantial overlap of the opposite spin interbands when the electron-electron interaction is considered within the Hartree-Fock approximation. In our study, we consider two different types of superlattices that present both spin instabilities that involve electrons from different Landau levels, as well as from the same, lowest Landau level. In each case, we solve the SDW gap equation numerically through an iterative procedure and study the dependence of the solution on the relevant system parameters. Our numerical estimates indicate that in the SDW ground state, the systems present a sizable spin polarization that is entirely controllable by external means, generating possible spintronics applications.

Table of Contents

List of Figures

Chapter 1

Introduction

Understanding the physics behind the collective behavior of interacting electron systems has always been a most interesting subject for both theoretical and experimental work, as such phenomena are a macroscopic picture of fundamental microscopic quantum mechanical properties. Illustrious examples of such collective behavior are superconductivity in metals and integer and fractional quantum Hall effect in two-dimensional semiconductors. In each case, under certain conditions, the Coulomb interaction between particles is drastically modified, its isotropic character in momentum space being replaced by a preferential coupling acting only between specific electron states. This long range off-diagonal order creates the premise for the formation of a broken symmetry phase that is associated with the collective behavior.

Originally introduced in 1959 to explain antiferromagnetism in Chromium [1, 2], spin density waves (SDW) are a state of an electron system described by a periodic spatially modulated spin polarization. This means that along certain spatial directions the collective spin orientation of the electrons varies continuously throughout the system. In Chromium, this situation is created by the Fermi surface nesting which creates an accidental spin degeneracy. More interestingly, in a series of refer-

ence papers [3, 4], Overhauser demonstrated that, within the Hartree-Fock approximation, the ground state energy of an electron system with weak correlations is lower in the SDW state than in the usual, paramagnetic, which has zero polarization, or ferromagnetic, which is fully polarized, states.

The physical origin of the SDW instability is the reduction in the total energy of the system when the exchange energy, the Coulomb interaction between parallel spins, becomes dominant when compared with the kinetic energy. Since even for a small increase in the spin polarization, which favors exchange, the whole Fermi surface of each spin species has to be modified, in a SDW state only a small portion of the paramagnetic Fermi surface is allowed to distort. This is realized by a preferential coupling between electrons of almost equal energy and of opposite spins, whose momenta are displaced, in the momentum space, by a vector $\vec{Q}$, the same for all the electron pairs that interact. The restriction on the electron momentum is compensated by the liberation of the spin which is allowed to depart from the standard up-down representation.

SDW's are closely related with modulated density distributions, called charge density waves (CDW). In a typical CDW/SDW state, the spin-dependent particle density is described by

$$\begin{aligned} n_\uparrow &= \frac{n}{2} + A\cos\left(\vec{Q}\cdot\vec{r} + \frac{\phi}{2}\right) , \\ n_\downarrow &= \frac{n}{2} + A\cos\left(\vec{Q}\cdot\vec{r} - \frac{\phi}{2}\right) , \end{aligned} \tag{1.1}$$

where A is the amplitude of the wave, and ϕ is the relative phase of the up-spin and down-spin density oscillations. A pure CDW corresponds to $\phi = 0$, whereas a pure SDW has $\phi = \pi$.

In real systems, however, the Hartree-Fock approximation does not suffice.

Dynamic effects associated with the short range Coulomb interaction, correlations have to be considered. Whereas in the Hartree-Fock approximation, the SDW and CDW phase have equal energy, when correlations are included, it was shown that CDW phases are favored [5]. Several simple metals, potassium (K) in particular are considered good candidates for exhibiting a CDW ground state, a prediction supported by a series of relevant experiments [6].

Because in normal metals the electron density and energy band structure cannot be easily modified, the study of spin/density instabilities in artificially grown semiconductor heterostructures has been predominant in the recent years. These systems present the advantage that the electron density, which determines the strength of the Coulomb interaction, can be varied over a large range by tuning experimentally controllable parameters.

The simplest semiconductor structure is a quantum well, an artificially created potential trap that confines particles to two dimensions (2D), restricting their motion in a planar region. Technically, this situation is realized where a thin region of a narrow gap semiconductor is sandwiched between layers of a wide band gap semiconductor or surrounded by a wide band gap semiconductor. The effects of the quantum confinement take place when the quantum well thickness becomes comparable with the de Broglie wavelength of the carriers (generally electrons and holes), leading to the quantization of the electron levels along the direction perpendicular to the interface. The system of reference for a standard quantum well is the interface between GaAs and AlGaAs, which is also considered here.

The quenching of the third degree of freedom, enhances the electron interaction, especially the correlation part which is associated with the short range Coulomb potential, leading to the realization of special quantum phases, such as the integer and the fractional quantum Hall effect [7]. At low densities Wigner crystallization

was shown to occur [8].

In the presence of a high magnetic field, perpendicular to the interface, the orbital electron motion is quantized and the energy spectrum is discrete, formed by a sequence of Landau levels. When the width of the quantum well is taken into account the Landau levels are broadened into minibands. Since, in GaAs the effective magnetic moment of the electrons is very small, in the presence of a magnetic field B perpendicular to the interface, the electron system is unpolarized, the Zeeman splitting is negligible. When the field is tilted with respect to the normal to the surface, the energy level structure is determined by the interplay between the cyclotron energy, which represents the spacing between two consecutive Landau levels, $\hbar\omega_c = \frac{\hbar eB}{m^*c}$ and the Zeeman splitting $2\gamma^*B$. (m^* is the effective band mass and γ^* is the effective gyromagnetic factor expressed in Bohr magnetons). The two energies can become comparable considering that $\hbar\omega_c$ depends on the normal component of the field, whereas the Zeeman splitting depends on the magnitude. If $2\gamma^*B \ll \hbar\omega_c$, the spectrum is characterized by a sequence of Landau levels, and each of Landau levels displays a small spin splitting . In the opposite case, $2\gamma^*B \gg \hbar\omega_c$, the spectrum consists of widely separated spin-up and spin-down components, each presenting a fan of Landau levels, a situation realized in magnetic semiconductors. Introducing additional degrees of freedom associated with spin, layer, or sub- band index, the 2D electron gas in the presence of a strong external magnetic field is known to have an extremely rich quantum phase diagram [9],[10].

The first attempts to initiate the formation of SDW phases in semiconductor structures with controllable parameters, such as a single quantum well, were done in Ref. [11]. As we discuss in Ch. 3, it was found that, in the presence of a magnetic field, the electron gas undergoes an abrupt paramagnetic to ferromagnetic transition and does not sustain a stable SDW ground state. This negative result was very important

since it revealed that additional degrees of freedom have to be considered such that the many-body interaction can drive a phase transformation from paramagnetic or ferromagnetic to a SDW.

This can be accomplished by considering double quantum well systems (DQWS), realized by parallel aligning two identical quantum wells. The two wells are coupled by a finite electron tunneling probability. When tunneling between wells occurs [12], the energy levels split into symmetric and antisymmetric states, their splitting Δ_{SAS} being proportional to the tunneling probability. The competition of the different ground states realized in the presence of a magnetic field is controlled by the relation between the Coulomb interaction energy, the spin splitting and the $S - A$ splitting caused by inter-layer tunneling [13].

In the simplest single particle picture, each Landau level has four sub-levels originating from the spin and sub-band splittings. With increasing spin splitting a transition occurs from a spin unpolarized ground state with antiparallel spin orientations of occupied sub-levels to a ferromagnetic one with parallel spins when the Zeeman energy $\mu_g B$ is equal to the symmetric -antisymmetric splitting Δ_{SAS}. Experimentally this transition was observed to occur at a Zeeman energy significantly smaller than Δ_{SAS} [14], pointing out the importance of many-body effects, a subject we review in Ch. 4.

Because of the Coulomb repulsion, the mixing of symmetric and antisymmetric states with opposite spin directions generates a new ground state whose magnetic structure is that of a canted antiferromagnet [15]. At low, but experimentally accessible electron density ($\sim 0.7 \times 10^{11} cm^{-2}$) a novel exchange-correlation driven zero-field electronic phase transition was discovered. This occurs when the inter-sub-band spin-density-excitation gap vanishes because the excitonic vertex correction becomes larger than the single-particle symmetric-antisymmetric energy gap, Δ_{SAS},

in the system. At this point the system becomes unstable with respect to the spontaneous formation of zero-energy spin-density excitation, or equivalently, many body triplet exciton pairs [16].

The investigation of the magnetic phase diagram of an electron system in the presence of a magnetic field was continued by allowing for more degrees of freedom, specifically a quantized momentum along the $\hat{z}$ axis. The physical system that favors this type of investigation is a superlattice (SL). A superlattice is obtained by aligning a large number of quantum wells along a given spatial direction [17]. Such structures possesses periodicity both on the scale of each layer's crystal lattice and on the scale of the alternating layers. The SL constant lies typically in the range of tens to hundreds of angstroms, shorter than the electron mean free path, but longer than the lattice spacing. The superlattice periodicity modifies significantly the band structure of the layered semiconductors, creating minizones in wave vector space and sub-bands in energy.

Technically, there are two typical semiconductor superlattice. In type I superlattices, typified by GaAs-$Ga_{1-x}Al_xAs$, the conduction and valence bands are widely separated, so that the sub-band energies and their dispersion relations can be obtained by wave function matching along the direction perpendicular to the superlattice layers, using simple plane waves, and treating electrons and holes separately. The result of this approximation is presented in Fig. 1.1, where both electron and holes are showed to be confined in the GaAs region, as indicated in the shaded areas. In the figure, 1 and 2 indicate the first and second host semiconductors, while c, v mark their conduction and valence bands, respectively. In type II superlattices, typified by InAs-GaSb, the conduction band of one material is close to the valence band of the other as shown in Fig. 1.2, and strong band interaction occurs. This situation can be solved by matching the Bloch functions of electrons and holes, assumed cou-

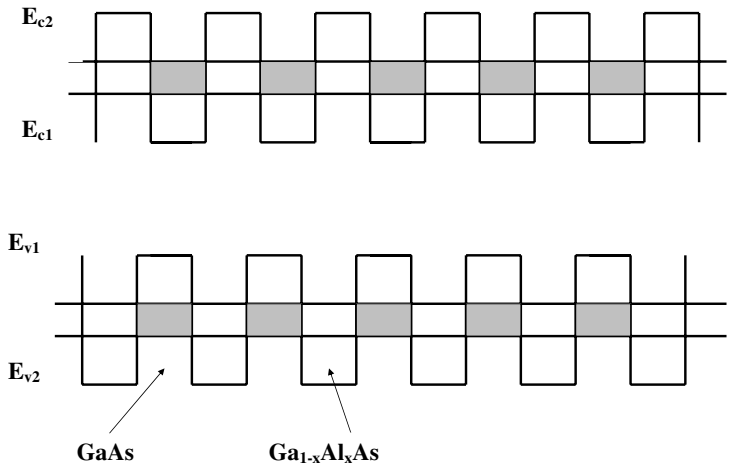

Figure 1.1: Energy Bands In a Type I Superlattice

pled. In the resulting energy spectrum, the electrons mainly exist in InAs . while the holes reside in GaSb. The spatial separation has obvious consequences on the optical properties, absorption frequencies and carrier lifetimes. Another important difference is the existence of an energy range between E_{c1} and E_{v2} in the superlattices of InAs-GaSb, where both electrons and holes states can be present simultaneously. As the layer thickness is increased, $E_{gs} = E_{1e} - E_{2h}$ decreases and may become zero and eventually negative, in contrast to the situation in GaAs-$Ga_{1-x}Al_xAs$ where E_{gs} is limited to the energy gap of $GaAs$.

The electronic and magnetic properties of semiconductor super lattices can be intentionally varied by changing their quantum well structures, tuning the electron density and band structure over a wide range of values. Generally speaking, the semiconductor superlattice is characterized by a high intrinsic electron mobility, smaller effective mass, and larger g factor than all binary $III - V$ semiconductors.

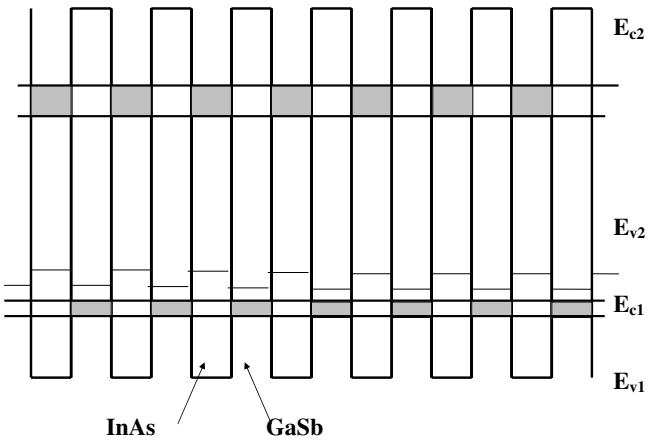

Figure 1.2: Energy Bands In a Type II Superlattice

All these characteristics translate into unique transport properties at low temperature [18], making them suitable for device applications such as high-speed transistors [19] and sensitive magnetoresistors [20].

In this project we employ the parametric flexibility of semiconductor superlattices to study the existence of stable spin density wave phases. The intuition behind this project is that a superlattice is nothing other than a one-dimensional crystal, whose properties, however, can be adjusted, generating a unique opportunity to investigate the interaction that underlies the occurrence of a SDW phase. To achieve this goal we analyze the existence of SDW phases in two different semiconductor heterostructures. In the first case, the superlattice unit cell is composed of a single quantum well and we rely on the cross-over of two Landau levels to obtain a many-body interaction strong enough to drive a magnetic phase transition to a SDW state. By using the external magnetic field, we depart from the idea of a spontaneous for-

mation of a SDW phase as predicted to develop in the simple electron gas. We try to minimize this influence by studying the possible existence of a SDW within the same Landau level by considering a different superlattice system, whose unit cell consists of a double-quantum well system. The required energy structure, in this case, is realized by the intra-unit-cell tunneling and Zeeman splitting.

In both cases, we develop the microscopic theory that underlies the formation of SDW and provide numerical solutions that indicate the existence of a finite spin polarization spatially modulated along the superlattice axis.

Chapter 2

Spin Density Waves In An Interacting Electron System

The ground state of an interacting electron system is essentially determined by its density, since the fundamental many-body interaction, the Coulomb repulsion, is dependent on the number of particles that participate. In the standard representation, the electron system is described by a collection of N particles inside a volume V superimposed on a positive background. The electronic wave functions are normalized spinors of wave-vector $\vec{k}$ and spin function χ_σ, where the latter is either one of the eigenstates of the $\hat{z}$ component of the spin operator $|\uparrow>$ and $|\downarrow>$ associated with eigenvalues $\sigma = +1$ and $\sigma = -1$ respectively:

$$\varphi_{\vec{k},\sigma}(\vec{r}) = \frac{1}{\sqrt{V}} e^{i\vec{k}\cdot\vec{r}} \chi_\sigma \ . \tag{2.1}$$

The single non-interacting electron energy is $\epsilon_{\vec{k},\sigma} = \frac{\hbar^2 \vec{k}^2}{2m}$.

The many-body Hamiltonian of the system, is written, in the second quantization language that introduces the creation and destruction operators for the electron

states, $c^{\dagger}_{\vec{k}}$ and $c_{\vec{k}}$, respectively, as

$$H = \sum_{\vec{k}} \epsilon_{\vec{k}} c^{\dagger}_{\vec{k}} c_{\vec{k}} - \frac{1}{2} \sum_{\vec{q},\vec{k},\sigma\vec{k}',\sigma'} v(\vec{q}) c^{\dagger}_{\vec{k}-\frac{\vec{q}}{2},\sigma} c^{\dagger}_{\vec{k}'+\frac{\vec{q}}{2},\sigma'} c_{\vec{k}'-\frac{\vec{q}}{2},\sigma'} c_{\vec{k}+\frac{\vec{q}}{2},\sigma} \tag{2.2}$$

where the first term is the kinetic energy of the electrons, while the second term describes the Coulomb interaction between two electrons that exchange a momentum $\vec{q}$. $v(\vec{q}) = 4\pi e^2/q^2$ is the matrix element of the Coulomb interaction between states given by Eq. (2.1).

The challenge involved in solving the quantum mechanical problem anchored by the above Hamiltonian is finding an exact solution for the interaction part. Therefore, over the past sixty years various methods of approximation have been developed, which we briefly review below.

In the simplest picture, an electron experiences just an averaged field created by all the other electrons. This statement defines the mean-field approximation or the random phase approximation (RPA), in which the full interaction potential is replaced by a sum of single particle terms,

$$\tilde{V}_{\vec{k},\sigma} = \sum_{\vec{k},\vec{q}} v(q) c^{\dagger}_{\vec{k}-\frac{\vec{q}}{2},\sigma} c_{\vec{k}+\frac{\vec{q}}{2},\sigma} \sum_{\vec{k}',\sigma} < c^{\dagger}_{\vec{k}'-\frac{\vec{q}}{2},\sigma'} c_{\vec{k}'+\frac{\vec{q}}{2},\sigma'} >_0 \ , \tag{2.3}$$

where $< \ldots >_0$ represents the average on the ground state of the system. The latter is itself dependent on the solution obtained for the electron motion, leading to a self-consistent set of equations. Eq. (2.3) represents the interaction between an electron and an average density of other electrons in the system defined by

$$\Delta n(\vec{q}) = \sum_{\vec{k}'} < c^{\dagger}_{\vec{k}'-\frac{\vec{q}}{2},\sigma'} c_{\vec{k}'+\frac{\vec{q}}{2},\sigma'} >_0 \ . \tag{2.4}$$

The next level of approximation of the many-body interaction is to consider the Pauli exclusion principle which prohibits two electrons with the same quantum numbers, here the wave-vector $\vec{k}$ and spin σ, of occupying the same spatial coordinates. In this approximation, the ground state average of the four operator product involved in the interaction part of Eq. (2.2) is replaced by a product of two averages of two operators estimated on the same ground state. Thus, by applying Wick's theorem,

$$\begin{aligned} & < c^{\dagger}_{\vec{k}-\frac{\vec{q}}{2},\sigma} c^{\dagger}_{\vec{k}'+\frac{\vec{q}}{2},\sigma'} c_{\vec{k}'-\frac{\vec{q}}{2},\sigma'} c_{\vec{k}+\frac{\vec{q}}{2},\sigma} >_0 \simeq < c^{\dagger}_{\vec{k}-\frac{\vec{q}}{2},\sigma} c_{\vec{k}+\frac{\vec{q}}{2},\sigma} >_0 < c^{\dagger}_{\vec{k}'+\frac{\vec{q}}{2}^{\dagger},\sigma'} c_{\vec{k}'-\frac{\vec{q}}{2},\sigma'} >_0 \\ - & < c^{\dagger}_{\vec{k}-\frac{\vec{q}}{2},\sigma} c_{\vec{k}'-\frac{\vec{q}}{2},\sigma'} >_0 < c^{\dagger}_{\vec{k}'+\frac{\vec{q}}{2}^{\dagger},\sigma'} c_{\vec{k}+\frac{\vec{q}}{2},\sigma} >_0 \ . \end{aligned} \tag{2.5}$$

The first term on the right-hand-side of Eq. (2.5) is non-zero only for $\vec{q} = 0$. It represents the divergent direct interaction which is fully compensated by the interaction with the positive background. The value of the second term is entirely dependent on the nature of the ground state, as yet unknown. So at this point, an *apriori* assumption is needed to be made about the ground state of the system.

In the simplest picture, two opposite-spin electrons share the same state described by the same wave-vector $\vec{k}$. Thus, in the paramagnetic state electrons occupy states of progressively increasing energy in the 3D momentum space, up to the maximum wave-vector k_F, related to the electron density by

$$n = \frac{k_F^3}{3\pi^2} \ . \tag{2.6}$$

This is the familiar Fermi sphere description of the Fermi liquid in the 3D momentum space. Consequently, when this happens, the only non-zero value for the average of

two operators in Eq. (2.5) occurs when the two electrons have parallel spins,

$$< c^{\dagger}_{\vec{k'}+\frac{\vec{q}}{2}^{\dagger},\sigma'} c_{\vec{k}+\frac{\vec{q}}{2},\sigma} >_0 = < c^{\dagger}_{\vec{k'}+\frac{\vec{q}}{2}^{\dagger},\sigma'} c_{\vec{k}+\frac{\vec{q}}{2},\sigma} >_0 \, \delta_{\vec{k}\vec{k'}} \delta_{\sigma\sigma'} = n^0_{\vec{k}+\frac{\vec{q}}{2},\sigma} \delta_{\sigma\sigma'} \tag{2.7}$$

where $n^0_{\vec{k}}$ is the occupation number of the state indexed by $\vec{k}$. At low temperatures, the distribution function is a step function, $n^0_{\vec{k}} = \theta(k_F - k)$. Thus, the Hartree-Fock exchange potential is

$$V_{\vec{k},\sigma} = -\sum_{\vec{q}} v(\vec{q}) n^0_{\vec{k}+\vec{q},\sigma} \, . \tag{2.8}$$

Eq. (2.8) allows the separation of the original Hamiltonian of the problem, Eq. (2.2) into a sum of one-particle energies given by,

$$\tilde{\epsilon}_{\vec{k},\sigma} = \epsilon_{\vec{k},\sigma} - V_{\vec{k},\sigma} \, . \tag{2.9}$$

The Hartree-Fock energy per electron in the paramagnetic state is obtained by summing all the energies Eq. (2.9) in the momentum space, leading to

$$\frac{W}{N}_p = \frac{3\hbar^2 k_F^2}{10m} - \frac{3e^2 k_F}{4\pi} \, , \tag{2.10}$$

From Eq. (2.9) it is also clear that, within the Hartree-Fock approximation, minimizing the total energy of the system is a competition between the kinetic energy term and the exchange potential $V_{\vec{k}\sigma}$.

An alternative configuration in the momentum space for the same density N, is obtained by allowing only one electron on each state described by momentum $\vec{k}$. In the ferromagnetic state, electrons occupy single spin states inside a sphere within

a radius of $2^{\frac{1}{3}}k_F$. The HF energy per electron of the ferromagnetic state is:

$$\frac{W}{N}_f = 2^{\frac{1}{3}}\frac{3\hbar^2 k_F^2}{10m} - 2^{\frac{1}{3}}\frac{3e^2 k_F}{4\pi} \ . \tag{2.11}$$

Eqs. (2.10) and (2.11) indicate that the ferromagnetic state has lower energy than the paramagnetic state when

$$k_F < \frac{5me^2}{(2^{\frac{1}{3}}+1)2\pi\hbar^2}. \tag{2.12}$$

Consequently, a high density electron gas would be paramagnetic and a low density one would be ferromagnetic. This criterion was first derived by Bloch [21].

If in Eq. (2.5), however, one imagines that there exists such a ground state for which

$$< c^{\dagger}_{\vec{k'}+\frac{\vec{q}}{2},\sigma'} c_{\vec{k}+\frac{\vec{q}}{2},\sigma} >_0 \neq 0 \ , \tag{2.13}$$

when $\sigma \neq \sigma'$, the outcome of the HF approximation is entirely different.

This concept was first introduced by Overhauser [4],[22] who showed that the Hartree-Fock ground state of a Fermi gas with Coulomb interactions is not the familiar sphere of occupied momentum states, but rather a state in which there are large static spin density waves and in which large energy gaps exist in the single-particle excitation spectrum.

The fundamental intuition behind this proof is that a degeneracy that occurs between energy levels occupied by opposite spin electrons favors a pairing between states $|\vec{k},\uparrow>$ and $|\vec{k}+\vec{Q},\downarrow>$ that minimizes the total energy by increasing the negative exchange energy with a relatively low increase in the kinetic energy. In a SDW state the electron gas has a finite fractional polarization at each point $\vec{P}(\vec{r})$ whose direction

varies continuously with the position,

$$\vec{P} = P(\hat{x}\cos Qz + \hat{y}\sin Qz)\ . \tag{2.14}$$

Here the axis of the SDW is taken to be $\hat{z}$.

In the Overhauser theory, the spin polarization of the above form leads to an off-diagonal contribution to the single-electron exchange potential, Eq. (2.13) that can be written as:

$$V^{'} = -g \begin{pmatrix} 0 & e^{-iQz} \\ e^{iQz} & 0 \end{pmatrix}. \tag{2.15}$$

For this potential, the single particle Schrödinger equation is written as:

$$\left[\frac{\vec{P}^2}{2m} + V^{'}\right]\psi_k = E_k\psi_k\ . \tag{2.16}$$

The energy eigenvalues are,

$$E_k^{+} = \frac{1}{2}(\epsilon_k + \epsilon_{k+Q}) \pm \left[\frac{1}{4}(\epsilon_k - \epsilon_{k+Q})^2 + g^2\right]^{\frac{1}{2}}\ . \tag{2.17}$$

where ϵ_k is the energy of an electron of momentum $\mathbf{k}$ written within the Hartree-Fock approximation. The associated wave functions for the lower branch is

$$\varphi_k = \frac{1}{V^{\frac{1}{2}}}[|\uparrow> \cos\theta e^{ik\cdot r} + |\downarrow> \sin\theta e^{i(k+Q)\cdot r}]\ , \tag{2.18}$$

where

$$\cos\theta(k) \equiv \frac{g}{[g^2 + (\epsilon_k - E_k)^2]^{\frac{1}{2}}}\ , \tag{2.19}$$

The wave function of the upper branch is,

$$\varphi_k = \frac{1}{V^{\frac{1}{2}}} \left[|\uparrow> \cos\left(\theta + \frac{\pi}{2}\right) e^{i\vec{k}\cdot\vec{r}} + |\downarrow> \sin\left(\theta + \frac{\pi}{2}\right) e^{i(\vec{k}+\vec{Q})\cdot\vec{r}} \right] . \tag{2.20}$$

The single-particle energy spectrum is shown in the Fig. 2.1.

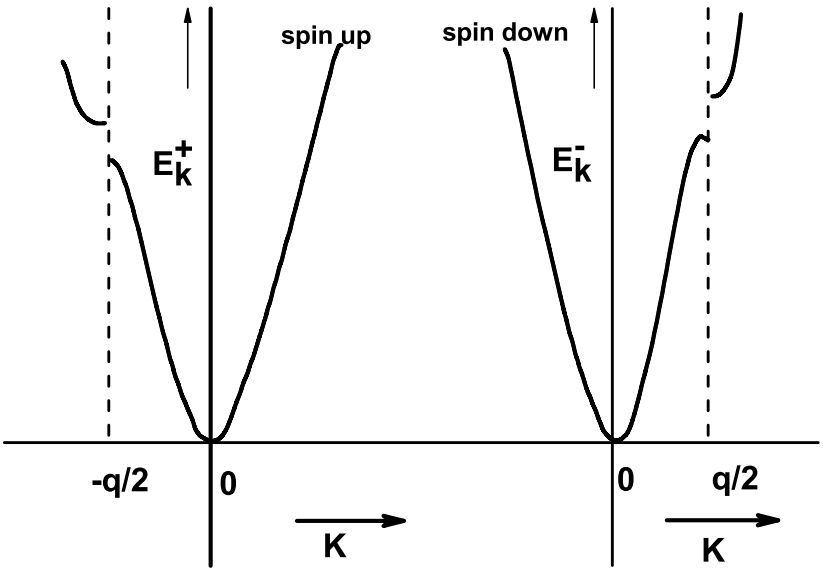

Figure 2.1: An Electron Gas With Giant Spiral Spin Density Wave

A more clear demonstration for the spin-density wave formation is shown in Fig. 2.2 The spin-down have been displaced by Q to the left of the spin-up branch. Only the lower branch states are occupied in a SDW ground states.

The physical reason behind the lower energy of the SDW states is that the increase in exchange energy is larger than the increase in the kinetic energy.

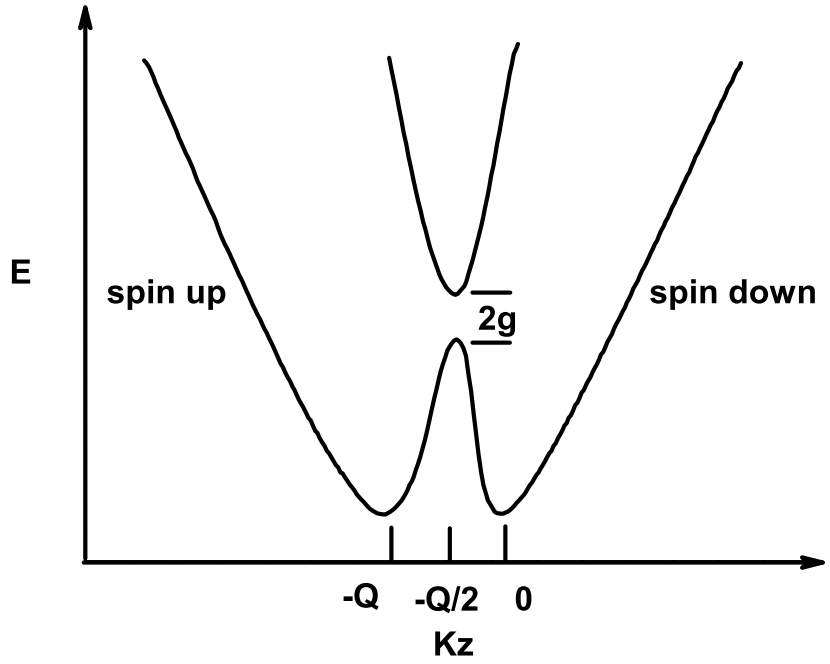

Figure 2.2: Single-particle Energy Level Spectrum In a Spiral Spin Density Wave.

Chapter 3

Spin Instabilities In A Single Quantum Well

3.1 Single Electron In A Magnetic Field; Landau Level Quantization

In the presence of a magnetic field $\vec{B}$, the Hamiltonian of a single electron of momentum $\vec{P} \equiv (P_x, P_y, P_z)$ is written:

$$H = \frac{[\vec{P} + e\vec{A}]^2}{2m} \ . \tag{3.1}$$

where $\vec{A}$ is the magnetic vector potential associated with $\vec{B}$. In the usual, Landau gauge, for a magnetic field along the $\hat{z}$ direction, $\vec{A} = (0, Bx, 0)$. The resulting Hamiltonian is:

$$H = \frac{[{P_x}^2 + (P_y - eB_x)^2]}{2m} \ . \tag{3.2}$$

A solution to the Schrödinger equation, $H\psi = E\psi$ can be written as $\psi = e^{i(k_y y)}u(x)$, where $u(x)$ satisfies the following equation:

$$\left[-\frac{\hbar^2}{2m}\frac{d^2}{d^2x} + \frac{m\omega_c^2}{2}(l^2k_y - x)^2\right]u(x) = \left[E - \frac{\hbar^2 k_z^2}{2m}\right]u(x) \ , \tag{3.3}$$

where $\omega_c = \frac{eB}{m}$ is the cyclotron frequency and $l^2 = \frac{c\hbar}{eB}$ is the magnetic length. As one recognizes the equation of motion of a harmonic oscillator of frequency ω_c displaced from the origin by $x_0 = k_y l^2$, $u_n(x)$ is

$$u_n(x + l^2k_y) = \frac{1}{\sqrt{2^n\sqrt{\pi}n!}}e^{-\frac{(x+l^2k_y)^2}{2l^2}}H_n(\frac{x}{l} + lk_y) \ , \tag{3.4}$$

Where $H_n(x)$ is n^{th} order Hermite polynomial. The corresponding eigenvalues are

$$\epsilon_n = \hbar\omega_c\left(n + \frac{1}{2}\right) \ , \quad (n = 0, 1, 2, \ldots), \tag{3.5}$$

which defines the quantized energy levels associated with the motion in the $x - y$ plane, called the Landau levels.

For electrons in a quantum well assumed to be infinitesimally thick, the wave function is usually written

$$\psi_{n,k_y}(x, y) = \frac{1}{\sqrt{L}}e^{ik_y l}u_n(x + k_y l^2) \ , \tag{3.6}$$

where the normalization is done by assuming periodic boundary conditions for k_y in a sample whose dimension along the $\hat{y}$ direction is L. In this case, k_y assumes a continuous spectrum, $k_y = \frac{2\pi}{L}j$, with $j \in \left(-\frac{L}{2}, \frac{L}{2}\right)$.

3.2 Excitonic Instabilities

In the following discussion we consider an electron system confined within a GaAs quantum well. On account of the very small gyromagnetic factor in GaAs, the Zeeman splitting of the Landau levels is negligible. This situation can be changed by tilting the magnetic field under an angle with respect to the normal to the plane. It is then possible to correlate a comparable Zeeman splitting, which depends on the magnitude of the field, with a comparable Landau splitting that depends on the normal component of the field. Then the energy difference in the same Landau levels can be distinguished by the presence of the Zeeman interaction. In Fig. (3.1) we describe this energy level sequence.

The low-lying excitations of this system occur when an electron from $|0,\uparrow>$

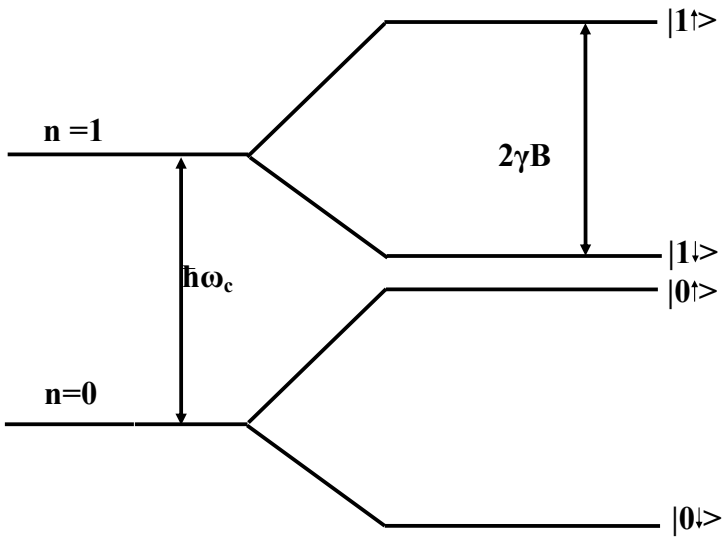

Figure 3.1: Diagram When Landau Levels And Zeeman Splitting Are Comparable

transitions on $|1,\downarrow>$ and leaves a hole behind. These electron-hole $(e-h$)pairs or excitons are bound by mutual attraction [11], [23]. The singlet exciton forms when the electron is promoted to a higher Landau level without a change in spin, as shown in Fig. 3.2, leaving behind a hole of opposite spin. The triplet exciton involves the promotion of a carrier to the opposite spin state of either the same Landau level or a higher one as indicated in Fig. 3.3.

The stability of these excitations, is assured by a negative value of the total transition energy. In estimating the effects of the many-body interaction, the ratio of the Coulomb energy, of the order of e^2/l, to the cyclotron energy $\hbar\omega_c$ acts as a small parameter for a perturbation expansion of the interaction energy.

In the following study we calculate the excitation energies of spin-flip transitions that occur between $|0\uparrow>$ to $|1\downarrow>$, first discussed in Ref. [23]. The electron

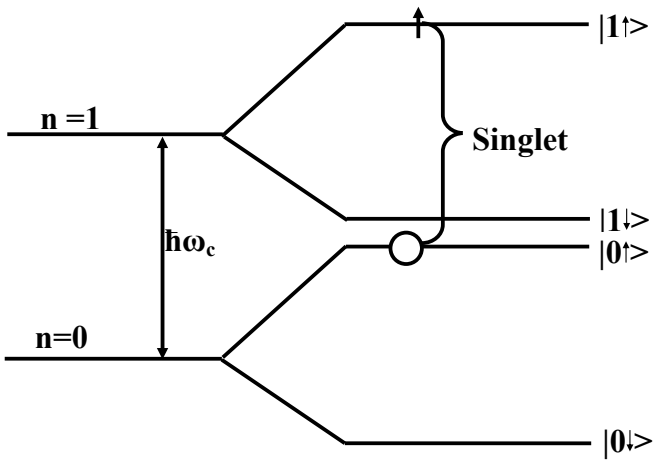

Figure 3.2: The Formation of Singlet Exciton

system is assumed to have a density n adjusted such that for a given intensity of the magnetic field the two lowest lying Landau levels are fully occupied. This condition is necessary to allow the application of the Hartree-Fock approximation in discussing the many-body interaction [24].

In the absence of electron-electron interactions, the energy of such an exciton would be $\epsilon \equiv \hbar(\omega_c - 2\gamma B)$. When electron-hole interactions are included, the triplet exciton forms when the the interactions exceed ϵ.

To calculate the interaction energy, we first express the Coulomb interaction matrix element that describes the scattering of an electron in state $|n, \vec{k}+\vec{q}, \sigma>$ with an electron in state $|m, \vec{k}+\vec{Q}, \sigma'>$ by exchanging a momentum $\vec{q}$, as described in Fig. 3.4.

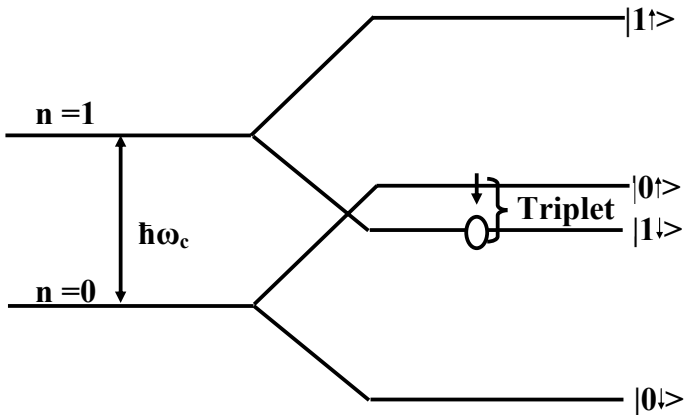

Figure 3.3: The Formation of Triplet Exciton

Thus, for the wave functions obtained in Eq. 3.6

$$v_{nm}(k,q,Q) = \int d^2r_1 \int d^2r_2 \psi^*_{n,\vec{k}+Q+\vec{q}}(\vec{r_1})\psi^*_{m,\vec{k}}(\vec{r_2})\frac{e^2}{|\vec{r_1}-\vec{r_2}|}\psi_{m,\vec{k}+\vec{q}}(\vec{r_2})\psi_{n,\vec{k}+\vec{Q}}(\vec{r_1}) \ . \tag{3.7}$$

The calculation is greatly simplified if one replaces the Coulomb interaction by its Fourier transform integral :

$$\frac{e^2}{|\vec{r}_1-\vec{r}_2|} = \frac{1}{(2\pi)^2}\int d^2q_0 \, \frac{2\pi e^2}{q_0} e^{i\vec{q}_0\cdot(\vec{r}_1-\vec{r}_2)} \ . \tag{3.8}$$

When Eq. (3.8) is inserted within Eq. (3.7) we can write

$$v_{nm}(\vec{k},\vec{q},\vec{Q}) = \sum_{\vec{q}_0}\frac{2\pi e^2}{q}\int d^2r_1 \psi^*_{n,\vec{k}+Q+\vec{q}}(\vec{r_1})e^{i\vec{q}_0\cdot\vec{r}_1}\psi_{n,\vec{k}+\vec{Q}}(\vec{r_1})\int d^2r_2\psi^*_{m,\vec{k}}(\vec{r_2})e^{-i\vec{q}_0\cdot\vec{r}_2}\psi_{m,\vec{k}+\vec{q}}(\vec{r_2}) \ . \tag{3.9}$$

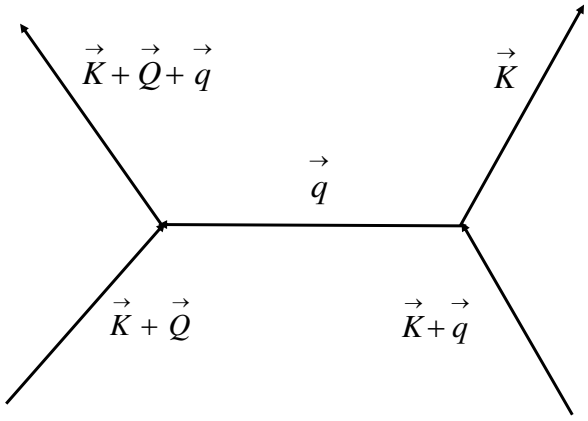

Figure 3.4: The Coulomb Interaction

In this form it is easy to recognize that

$$v_{nm}(\vec{k},\vec{q},\vec{Q}) = \frac{e^2}{2\pi}\int d^2q_0 I *_n (\vec{k}+\vec{Q},\vec{q},\vec{q}_0) I_m(\vec{k},\vec{q},\vec{q}_0) \ , \tag{3.10}$$

where

$$I_m(\vec{k},\vec{q},\vec{q}_0) = \int d^2r_2 \psi^*_{m,\vec{k}}(\vec{r_2}) e^{-i\vec{q}_0\cdot\vec{r}_2} \psi_{m,\vec{k}+\vec{q}}(\vec{r_2}) \ . \tag{3.11}$$

The integral I_m is straightforwardly performed by using the analytical form of the wavefunctions Eq. (3.6). We obtain

$$I_m(\vec{k},\vec{q},\vec{q}_0) = \frac{1}{L}\int_{-\infty}^{\infty} dy_2 e^{-i(q_{0y}-q_y)y_2} \int_{-\infty}^{\infty} dx_2 u_m\left(x_2+k_y l^2\right) e^{-iq_{0x}\cdot x_2} u_n\left[x_1+(k_y+q_y)l^2\right] \ . \tag{3.12}$$

Since, from the orthogonality condition

$$\frac{1}{L}\int_{-\infty}^{\infty} dx_2 e^{i(q_{0y}-q_y)x_2} = 2\pi\delta(q_{0y}-q_y) \ , \tag{3.13}$$

then,

$$I_m(\vec{k},\vec{q},\vec{q}_0) = \frac{\sqrt{2\pi}}{L}\delta(q_{0y}-q_y)\int_{-\infty}^{\infty} dx_2 u_m[x_2^2+(k_y+q_y)l^2] e^{-iq_{0x}x_2} u_m(x_2+k_y l^2) \ , \tag{3.14}$$

Finally, by employing the expression of $u_m(x)$ and by making a change of variable $x_2 + k_y l^2 \to x_2$, we write

$$I_m(\vec{k},\vec{q},\vec{q}_0) = \frac{\sqrt{2}}{2^m m! L}\delta(q_{0y}-q_y)\int_{-\infty}^{\infty} dx_2\, e^{-\frac{x_2^2+(x_2+q_y l^2)^2-iq_{0x}(x_2-k_y l^2)}{2l^2}} H_n(x_2/l) H_n(x_2/l+q_y l) \ . \tag{3.15}$$

Since we are interested only in the electrons on the $n = 1$ and $n = 0$ levels, we introduce the explicit expressions of H_0 and H_1 in the expression of I_m. With these,

from Eq. (3.10), one can immediately obtain

$$v_{nm}(q_y, Q_y) = \frac{e^2}{2\pi}\int_{-\infty}^{\infty} dq_{0x} \frac{1}{\sqrt{q_y^2 + q_{0x}^2}} e^{-\frac{l^2}{2}(q_y^2 + 2iq_{0x}Q_y + q_{0x}^2)} w_{nm}\left[(q_{0x}^2 + q_y^2)l^2\right] \ , \quad (3.16)$$

where

$$w_{nm}(x) = \left[\delta_{n0}\delta_{m0} + \left(1 - \frac{x}{2}\right)\delta_{n1}\delta_{m0} + \left(1 - \frac{x}{2}\right)^2 \delta_{n1}\delta_{m1}\right] \ . \quad (3.17)$$

The exciton energies are defined by the difference between the energy of an electron in the final configuration and the energy of the electron in the initial configuration. For the triplet exciton, which is formed as a result of a transition from $|0, \uparrow>$ to $|1, \downarrow>$, the electron loses the exchange energy with all other spin-up electrons of $|0 \uparrow>$ level, ϵ_{00}^x, while it gains the exchange energy with spin-down electrons of $|0 \downarrow>$, ϵ_{10}^x. In addition, it gains the attraction with the hole left behind, γ_{01}. The total energy associated with the transition is then

$$W = \epsilon - \epsilon_{00}^x + \epsilon_{10}^x + \gamma_{10} \ . \quad (3.18)$$

They are calculated within the Hartree-Fock approximation by summing over all the possible momenta transferred between the two electrons, $\vec{q}$. Thus, the interaction energy of an electron on level n with all the other electrons in level m, calculated in the Hartree-Fock approximation, is written as:

$$\epsilon_{nm}(\vec{k}, \vec{Q}) = -\sum_{\vec{q}} v_{nm}(\vec{q}, \vec{Q}) \ , \quad (3.19)$$

We remark that the exchange energy, wherein two electrons simply change the value of their momenta corresponds to $\vec{Q} = 0$ in the Coulomb diagram, Fig. 3.4, whereas in the expression of γ_{nm}, $\vec{Q}$ or rather its in-plane component Q_y remains a parameter.

It follows therefore, that

$$\epsilon^x_{nm}(\vec{k}) = -\sum_{\vec{q}} v_{nm}(\vec{q},0) \ , \tag{3.20}$$

while

$$\gamma_{01}(\vec{k},Q_y) = -\sum_{\vec{q}} v_{01}(\vec{k},\vec{q},\vec{Q}) \ . \tag{3.21}$$

By transforming the sum over $\vec{q}$ into an integral, $\sum_{\vec{q}} \rightarrow \frac{1}{(2\pi)^2}\int d^2\ q$, for the matrix elements calculated in Eq. (3.16) we obtain immediately

$$\epsilon^x_{00} = -\frac{e^2}{l}\sqrt{\frac{\pi}{2}} \ , \tag{3.22}$$

$$\epsilon^x_{01} = -\frac{e^2}{2l}\sqrt{\frac{\pi}{2}} = \frac{\epsilon^x_{00}}{2} \ , \tag{3.23}$$

$$\epsilon^x_{11} = -\frac{3e^2}{4l}\sqrt{\frac{\pi}{2}} = \frac{3\epsilon^x_{00}}{4} \ . \tag{3.24}$$

The electron-hole binding energy is:

$$\gamma_{10}(lQ_y) = -\frac{e^2}{l}\int_0^\infty dx e^{-\frac{x^2}{2}} J_0(lQ_y x)(1-\frac{x^2}{2}) \ , \tag{3.25}$$

where the integration variable is related to the in-plane momentum $\vec{q}$ by $x = l\sqrt{q^2_{0x}+q^2_y}$. J_0 is the zero-th order Bessel function whose argument represents the momentum of the exciton, Q_y.

From Eqs. (3.22),(3.23), and (3.25) we obtain the energy of a triplet exciton formed in the paramagnetic state as being equal to

$$W = \epsilon + \epsilon^{ex}_{00}\left[\frac{1}{2} - \gamma_{10}(lQ_y)\right] \ , \tag{3.26}$$

in which $\varepsilon = \hbar(\omega_c - \omega_s)$ and $R = lQ$ is related to the size of the exciton or the wave vector Q associated with the electron-hole separation [11]. The function $\gamma_{10}(x)$

reaches a maximum value of 0.573 for a value of its argument $lQ_y \cong 1.2$.

From Eq. (3.26) the stability of the exciton, that occurs when $W < 0$, is controlled by

$$\epsilon < 0.073|\epsilon_{00}^{x}| \; . \tag{3.27}$$

We now continue our analysis by considering a ferromagnetic ground state. The energy of a triplet exciton that can be formed by a spin-flip transition from $|1,\downarrow>$ to $|0,\uparrow>$ is given by the kinetic energy $-\epsilon$, the lost exchange with the electrons on $|0,\downarrow>$ and those on $|1,\downarrow>$ and the electron-hole binding energy. Thus, W' is

$$W^{'} = -\epsilon - \epsilon_{11}^{x} - \epsilon_{01}^{x} + \gamma_{01} = -\epsilon + 0.667|\epsilon_{00}^{x}| \; , \tag{3.28}$$

where we employed the numerical values of all the energies involved expressed in Eqs. (3.22), (3.23), and (3.25). The stability of the ferromagnetic exciton, realized for $W^{'} < 0$, is obtained when

$$\epsilon > 0.667|\epsilon_{00}^{x}| \; . \tag{3.29}$$

If one looks for the possibility of creating favorable conditions for the appearance of SDW phases, characterized by the simultaneous existence of triplet excitons formed from a paramagnetic or a ferromagnetic ground state, it is clear that these are not being realized in a quantum well since Eqs. (3.27) and (3.29) do not have a common solution. Thus, the conclusion of this analysis is that in a single quantum well the realization of spin instabilities on account of the many-body interaction triggers just a paramagnetic to ferromagnetic transition, but not a SDW state.

This outcome is supported by the many-body calculation done in Ref. [11], where it was found that within the unrestricted Hartree-Fock approximation, the SDW transition never occurs in a single well. The two stable solutions are the para-

magnetic and the ferromagnetic states. For $\epsilon < 0.073|\epsilon^x_{00}|$, the only stable HF solution is the ferromagnetic state, while for $\epsilon > 0.677|\epsilon^x_{00}|$ the paramagnetic state is stable. For $\epsilon \in (0.073, 0.677)|\epsilon^x_{00}|$ any of the two states can be realized depending on the density of the electron system, or more exactly, on the position of the Fermi level.

Chapter 4

Spin-Flip Transitions in the Lowest Landau Level

The gyromagnetic ratio of a bare particle, g, is defined as the ratio of its magnetic moment to its angular momentum. For an electron, the exact quantum mechanical calculation when only the spin momentum is involved generates a value $g = 2$. In interacting systems, however, g can depart considerably from the spin-only value because of the effects of spin-orbit coupling [25], band or dimensionality effects [26], [27]. Furthermore, in the presence of a weak magnetic field, that introduces a population imbalance $N_\uparrow \neq N_\downarrow$, interacting electrons at the Fermi surface are described by an effective g^* that differs from its band value on account of the exchange interaction, which is determined by the number of electrons with the same spin [28].

At strong fields, when the Landau quantization of the electron levels dominates the energy spectrum, the g factor enhancement can become extremely large whenever the Fermi level lies between spin split Landau levels [29], [30]. Such effects were explained by Ando and Uemura [31] who evaluated the self energy including Landau quantization in the static screening approximation. They pointed out that under

strong magnetic fields perpendicular to the surface, the density of states becomes discrete as a result of the complete quantization of the orbital motion. The difference in numbers of electrons with $\uparrow$ and $\downarrow$ spins, to which the enhancement is proportional, depends strongly on the position of the Fermi level. When it passes through the middle point of $(N, \uparrow)$ and $(N, \downarrow)$ levels (where N is the Landau levels index), the difference becomes maximum and consequently the g^* factor has a certain maximum value. When it lies at the middle point of $(N, \downarrow)$ and $(N+1, \uparrow)$ levels, the difference becomes minimum and the g^* factor oscillates with the increase of the total number of electrons.

The effective g^* factor, or equivalently, the effective magnetic moment of the electron $\gamma = g^*\mu_B$ (μ_B is the Bohr magneton), can be calculated by estimating the difference in the energy of the electron before and after a spin flip transition when its interaction with the rest of the electron gas is considered [28]. Thus, for an electron of momentum $\vec{k}$, the energy associated with a spin-flip is related to an "effective" Zeeman splitting, $2\gamma^* B$ in a magnetic field of intensity B, which is different from the natural splitting of the energy levels in a magnetic field, $2\gamma B$. The difference is a measure of the many-body interaction in the system.

In this chapter we discuss the effect of the electron-electron interaction on the effective gyromagnetic factor in the lowest Landau level. To create the energy spectrum that enables spin-flip transitions, we consider a double quantum well system (DQWS) whose components are coupled through weak tunneling. The γ factor is calculated from the many-body estimate of the spin-flip energy transition, and thus, is not only affected by the exchange interaction, but also depends on experimentally controlled system parameters such as the interlayer tunneling and the distance between the layers [32].

The system of interest is composed of two identical wells separated by a dis-

tance $2a$. They are considered to be infinitely attractive (essentially zero-width 2D planes) of potential $V(z) = -\lambda[\delta(z-a) + \delta(z+a)]$. A magnetic field $\mathbf{B}$ is applied under a finite angle with respect to the $\hat{z}$, perpendicular to the layers. This set-up permits the creation of a complex energy substructure inside the lowest Landau level, resulting from the competing effects of the Zeeman splitting, that can become quite substantial since it depends on the magnitude of the field, and the tunneling-induced splitting Δ_{SAS}.

While the electron motion in the $x-y$ plane continues to be described by Eq. (3.6), the $\hat{z}$ component of a single-electron wave function satisfies the following Schrödinger equation,

$$-\frac{\hbar^2}{2m}\nabla^2\zeta(z) - \lambda\left[\delta(z-a) + \delta(z+a)\right]\zeta(z) = 0\ . \tag{4.1}$$

Its solution can be simply obtained by a straightforward calculation. First, for $z \neq -a, a$, the wave function is written as:

$$\zeta(z) = \begin{cases} Ae^{\kappa z} & z \leq -a \\ Be^{\kappa z} + Ce^{-\kappa z} & z \in (-a, a) \\ De^{-\kappa z} & z \geq a \end{cases}\ , \tag{4.2}$$

where $\kappa = \sqrt{-2mE/\hbar^2}$, with $E < 0$ of a bound state. A, B, C, D are constants determined from the continuity of the function and its first derivative at $z = \pm a$. They satisfy a set of four homogeneous equations,

$$\begin{aligned} Ae^{-\kappa a} &= Be^{-\kappa a} + Ce^{\kappa a}\ , \\ De^{-\kappa a} &= Be^{\kappa a} + Ce^{-\kappa a}\ , \end{aligned}$$

$$\begin{aligned} \kappa A e^{-\kappa a} &= \kappa B e^{-\kappa a} - \kappa C e^{\kappa a} \ , \\ \kappa D e^{-\kappa a} &= \kappa B e^{\kappa a} - \kappa C e^{-\kappa a} \ . \end{aligned} \tag{4.3}$$

that admits a non-trivial solution only when its determinant is canceled.

$$\begin{vmatrix} 1 - \frac{m\lambda}{\kappa\hbar^2} & \frac{m\lambda}{\kappa\hbar^2} e^{-2\kappa a} \\ \frac{m\lambda}{\kappa\hbar^2} e^{-2\kappa a} & 1 - \frac{m\lambda}{\kappa\hbar^2} \end{vmatrix} = 0 \ . \tag{4.4}$$

The characteristic equation obtained in this way is

$$1 - \frac{m\lambda}{\kappa\hbar^2} = \pm \frac{m\lambda}{\kappa\hbar^2} e^{-2\kappa a} \ . \tag{4.5}$$

transcendental and a solution for κ can be obtained only approximatively. Within the first order in the tunneling probability, the exponential term is considered to be equal to that of the single infinite quantum well system, when $\kappa = m\lambda/\hbar^2$.

Consequently, the solution for the bound state energy

$$\epsilon_{S,A} = \epsilon_0 (1 \pm e^{-2\kappa a}) \ , \tag{4.6}$$

in which $\epsilon_0 = -\frac{m\lambda^2}{2\hbar^2}$ is the bound state energy in a single quantum well. The S subindex is associated with the plus sign, the symmetric level, while the A index is associated with the negative sign. Thus, as a result of the tunneling, the single electron level of a single well is split into a symmetric and an antisymmetric component to accommodate the additional degree of degeneracy introduced by the presence of a second well. The difference of these levels generates

$$\Delta_{SAS} = \epsilon_A - \epsilon_S = -2\epsilon_0 e^{-2\kappa a} \ . \tag{4.7}$$

The corresponding wave function is

$$\nu_{S,A}(z) = \sqrt{\frac{\kappa}{2}} \left(e^{-\kappa|z-a|} \pm e^{-\kappa|z-a|} \right) , \tag{4.8}$$

where the + sign corresponds to the symmetric (S) wave function, while $-$ to the antisymmetric (A) one.

The three dimensional motion of the electron is therefore described by

$$\psi_{S,A,k_y,\sigma}(x,y,z) = \nu_{S,A}(z)\phi_{k_y\sigma}(x,y) , \tag{4.9}$$

where $\phi_{k_y,\sigma}$ refers to the 2D motion in the lowest, $n = 0$, Landau level, as given by Eq. (3.6). Since this is the only level we consider, the index is not explicitly declared.

To calculate the effective gyromagnetic factor for spin-flip transitions in the lowest Landau level, we first establish the various energy configurations that can be realized when both the S-A energy difference, Δ_{SAS} realized on account of tunneling and Zeeman splitting $2\gamma B$ (here $\gamma = g\mu_B$) are considered.

If $2\gamma B \leq \Delta_{SAS}$, the $n = 0$ Landau level splits in four sublevels ordered as in Fig. (4.1), whereas when $2\gamma B \geq \Delta_{SAS}$, the sequence of levels is described by Fig. (4.2). In the first case, the ground state, which assumes the full occupancy of the lowest two sublevels, is paramagnetic, whereas in the second is ferromagnetic.

The effective γ factor is obtained by calculating the total energy associated with an electronic spin-flip transition. First, starting from the paramagnetic configuration, we consider spin-flips from $|S,\uparrow>$ to $|A,\downarrow>$. Similarly to what happens in a single quantum well, the total transition energy, defined as the electron energy after spin-flip minus the electron energy before spin-flip, involves the exchange energy of the electron before and after the transition, as well as the vertex corrections, repre-

sented by the bounding energy between the electron and the hole it leaves behind. In both cases the hole left behind by the electron has a spin parallel to that of the electron in its final state, and the $e-h$ complex is a spin triplet. Thus, we write

$$2\gamma_p^* B = \epsilon + \epsilon_{SA}^x - \epsilon_{SS}^x + \gamma_{SA} \ . \tag{4.10}$$

where $\epsilon \equiv (\Delta_{SAS} - 2\gamma B)$. In the process, the electron loses the exchange interaction with the other same spin electrons on $|S,\uparrow\rangle$ and gains the exchange energy with the electrons on $|S,\downarrow\rangle$ and the binding energy with the hole in $|S,\uparrow\rangle$. From the ferromagnetic configuration, we study the spin-flip transition between $|S,\uparrow>$ to $|A,\downarrow>$. The

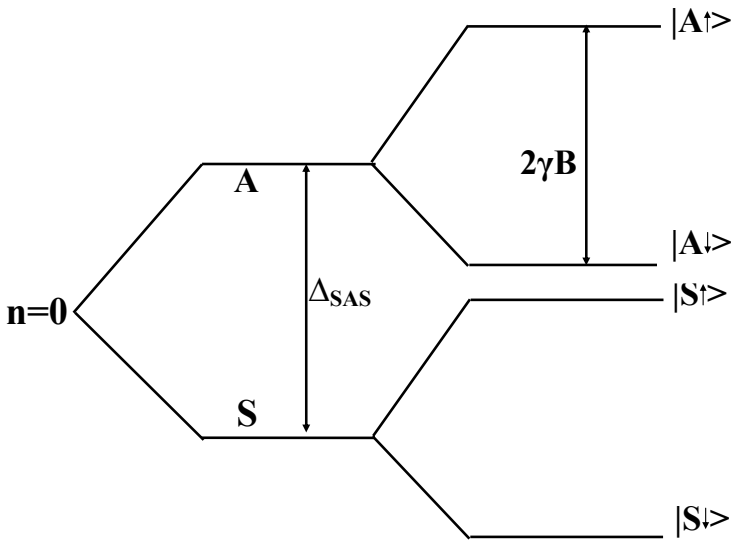

Figure 4.1: The Energy Level Distribution in the Lowest Landau Level of a Double Quantum Well in the Paramagnetic State

total energy involved in this transition is given by

$$2\gamma_f^* B = -\epsilon - \epsilon_{AA}^x - \epsilon_{AS}^x + \gamma_{AS} \ , \tag{4.11}$$

where we included the lost exchange interaction with the electrons in $|A,\downarrow>$ and in $|S,\downarrow>$ and gained electron-hole binding energy.

Two other spin-flip transitions are possible in this configuration. They couple energy levels separated by $2\gamma B$, leading to the creation of single excitons, $e-h$ pairs of opposite spins. In this case, the energy difference between the two levels participating in the transition is large, diminishing the influence of the many-body interaction. For this reason, we do not discuss these transitions.

The exchange energies, as well as the electron-hole binding energy are calcu-

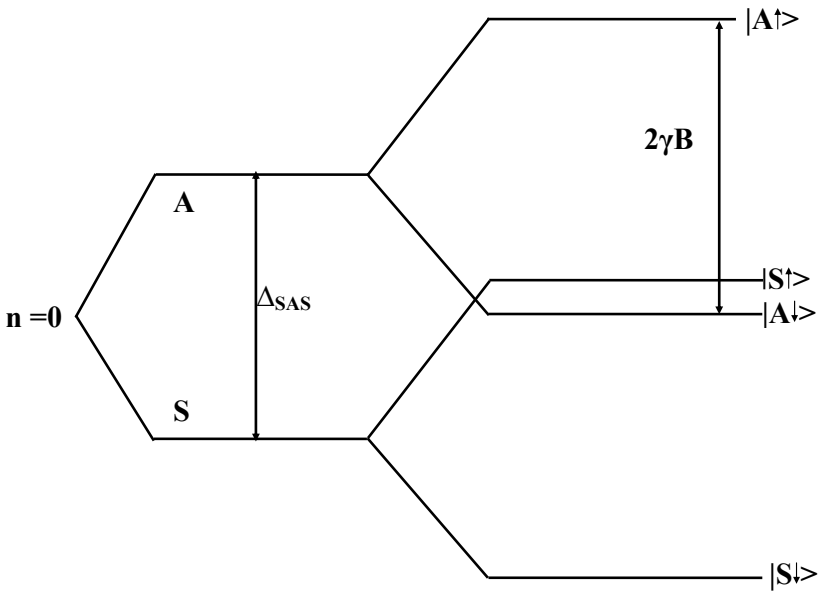

Figure 4.2: The Energy Level Distribution in the Lowest Landau Level of a Double Quantum Well in the Ferromagnetic State

lated starting from the Coulomb interaction matrix element, adapted to include the effect of electron motion along the $\hat{z}$ direction. As in the 2D case, we consider two electrons of incident momenta $\vec{k}+\vec{Q}$ and $\vec{k}+\vec{q}$ that interact via the Coulomb interaction by exchanging the momentum $\vec{q}$. The Coulomb interaction matrix element, given in Eq. 3.7 for a single well, becomes

$$v_{\alpha,\beta}(\vec{k},\vec{q},\vec{Q}) = \int d^3r_1 \int d^3r_2 \psi^*_{\alpha,\vec{k}}(\vec{r}_1)\psi^*_{\beta,\vec{k}+\vec{Q}+\vec{q}}(\vec{r}_2)\frac{e^2}{|\vec{r}_1-\vec{r}_2|}\psi_{\beta,\vec{k}+\vec{Q}}(\vec{r}_2)\psi_{\alpha,\vec{k}+\vec{q}}(\vec{r}_1) \ , \tag{4.12}$$

where α,β are either S (symmetric) or A (antisymmetric) indices. The calculation is easily performed by replacing the Coulomb interaction by its Fourier transform. To account for the tunneling occurring between the two wells, the correct representation of the Coulomb interaction would be that of a 2D Fourier transform of a 3D Coulomb interaction. Thus,

$$\frac{e^2}{|\vec{r}_1-\vec{r}_2|} = \sum_{\vec{q}_0}\frac{2\pi e^2}{q_0}e^{-q_0|z_1-z_2|} \ , \tag{4.13}$$

which expresses the fact that even though the electrons are confined to the 2D quantum wells they belong, the Coulomb interaction can mediate a certain overlap of the electron wave functions along the direction perpendicular to the planes. Here $\vec{q}_0$ is a two dimensional vector.

When Eq. (4.13) is inserted in Eq. (4.12) and the sum over $\vec{q}_0$ is replaced by an integral, we obtain:

$$\begin{aligned} v_{\alpha,\beta}(\vec{k},\vec{q},\vec{Q}) &= \frac{1}{(2\pi)^2}\int d^2q_0\frac{2\pi e^2}{q_0}\int d^3r_1\int d^3r_2\psi_{\alpha,\vec{k}}*(\vec{r}_1)\psi^*_{\beta,\vec{k}+\vec{Q}+\vec{q}}(\vec{r}_2)e^{-q_0|z_1-z_2|} \\ &\times \ \psi_{\beta,\vec{k}+\vec{Q}}(\vec{r}_2)\psi_{\alpha,\vec{k}+\vec{q}}(\vec{r}_1) \ . \end{aligned} \tag{4.14}$$

In this form, it is easy to see that when the wavefunctions described by Eq. (4.9) are used, the integrals over z_1 and z_2 separate, while the remaining 2D integrals

are entirely similar to those obtained in the single quantum well system. We write therefore, for the lowest Landau level, $n = 0$,

$$v_{\alpha,\beta}(q_y, Q_y) = \frac{e^2}{2\pi}\int_{-\infty}^{\infty} dq_{0x} \frac{1}{\sqrt{q_y^2 + q_{0x}^2}} e^{-\frac{l^2}{2}(q_y^2 + 2iq_{0x}Q_y + q_{0x}^2)} F_{\alpha,\beta}\left(\sqrt{q_{0x}^2 + q_y^2}\right) \ . \quad (4.15)$$

where we introduce the form factors $F_{\alpha,\beta}$ as the overlap integrals of the electron wave functions along the $\hat{z}$ direction,

$$F_{\alpha\beta}(q) = \int_{-\infty}^{\infty} dz_1 \int_{-\infty}^{\infty} dz_2 \nu_{1\alpha}(z_1)\nu_{2\beta}(z_2) e^{-q|z_1 - z_2|} \nu_{1\alpha}(z_1)\nu_{2\beta}(z_2) \ . \quad (4.16)$$

The particular forms of the form factors when the indices α, β correspond in turn to the symmetric (S) or antisymmetric (A) levels are obtained straightforwardly to be

$$\begin{aligned} F_{SS}(q) &= \left(\frac{\kappa}{2}\right)^2 \left\{ \frac{4}{(2\kappa+q)^2} + \frac{2}{\kappa(2\kappa+q)} + e^{-2\kappa a}\left[\frac{8}{\kappa q} + \frac{16}{(2\kappa+q)^2}\right.\right. \\ &+ \left.\left. \frac{4q}{\kappa(2\kappa+q)^2}\right] + e^{-2qa}\frac{32\kappa^2}{4\kappa^2 - q^2}\left[1 - \frac{2e^{-2\kappa a}}{q(\kappa+q)}\right]\right\} \ , \quad (4.17) \\ F_{SA}(q) &= \left(\frac{\kappa}{2}\right)^2 \left\{ \frac{4}{(2\kappa+q)^2} + \frac{2}{\kappa(2\kappa+q)} \right. \\ &+ \left. e^{-2qa}\left[16 + \frac{16q^2}{4\kappa^2 - q^2}\right]\right\} \ , \quad (4.18) \\ F_{AA}(q) &= \left(\frac{\kappa}{2}\right)^2 \left\{ \frac{4}{(2\kappa+q)^2} + \frac{2}{\kappa(2\kappa+q)} - e^{-2\kappa a}\left[\frac{8}{\kappa q} + \frac{16}{(2\kappa+q)^2}\right.\right. \\ &+ \left.\left. \frac{4q}{\kappa(2\kappa+q)^2}\right] - e^{-2qa}\frac{32\kappa^2}{2\kappa^2 - q^2}\left[1 - \frac{2e^{-2\kappa a}}{q(\kappa+q)}\right]\right\} \quad (4.19) \end{aligned}$$

Following Eqs. (3.19),(3.20), and (3.21), the exchange energies are written as:

$$\epsilon^x_{\alpha,\beta}(\vec{k}) = -\sum_{\vec{q}} v_{\alpha,\beta}(\vec{k}, \vec{q}, 0) \ , \quad (4.20)$$

while the electron-hole correlation energy is:

$$\gamma_{\alpha,\beta}(\vec{k},\vec{Q}) = -\sum_{\vec{q}} v_{\alpha,\beta}(\vec{k},\vec{q},\vec{Q}) \ , \tag{4.21}$$

Following the same integrating procedure outlined in the case of a simple quantum well, we obtain

$$\epsilon_{\alpha\beta}(\vec{k},\vec{Q}) = -\frac{e^2}{\pi l}\int_0^\infty dx\ x e^{-\frac{x^2}{2}} J_0(x, lQ_y) F_{\alpha,\beta}(x) \ . \tag{4.22}$$

We remark at this point that in the double-quantum well system, as in the case of a single well, there is no $\vec{k}$ dependence of the single electron interaction energy. However, the additional energy scale introduced by tunneling, generates a more interesting behavior.

Below we present the result of our numerical calculations of the effective γ factor that can be defined in connection with the two spin-flip transitions that can occur in the lowest Landau level when other means of introducing a symmetry breaking process, such as tunneling, are considered.

In Fig. 4.3, we show the dependence of γ^* (expressed in Bohr magnetons) on the tunneling probability $e^{-\kappa a}$ for a constant magnetic field B. As the tunneling increases, the coupling between the electrons in the two layers is enhanced leading to a large value for γ^*. A similar effect on γ^* has the decrease in the inter-layer distance, as seen in Fig. 4.4. At shorter distances, when the coupling is stronger, the effective gyromagnetic factor increases, signaling stronger interactions.

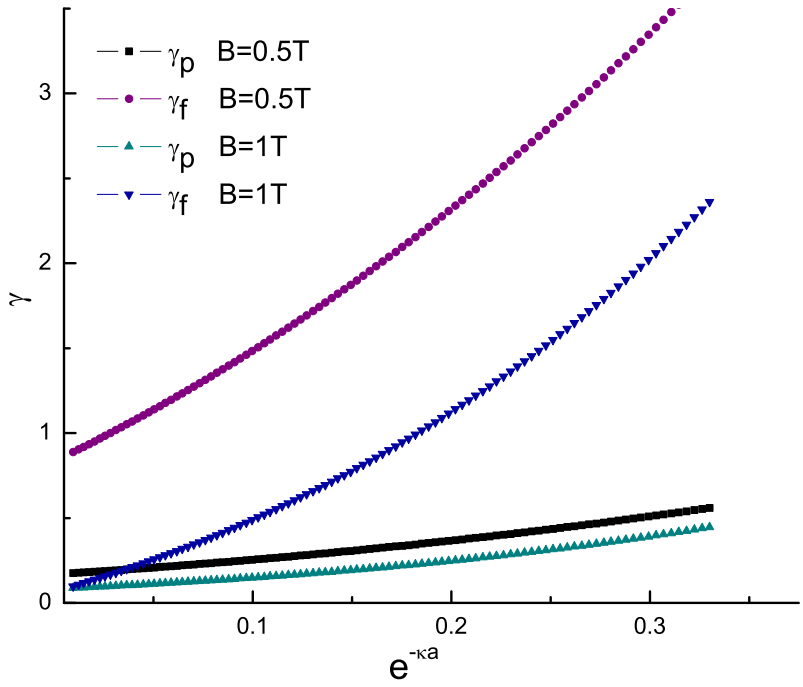

Figure 4.3: γ^* Dependence on the Tunneling Probability for a Constant Magnetic Field.

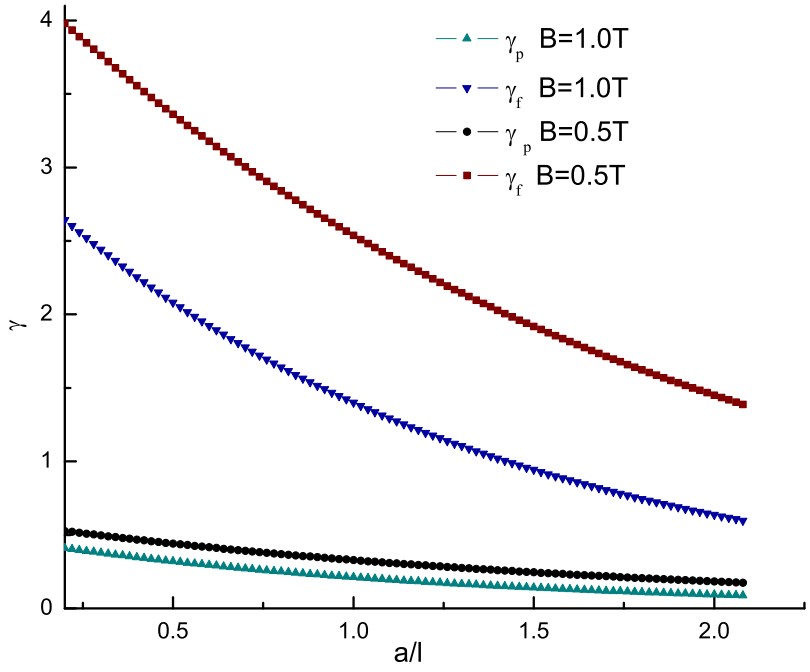

Figure 4.4: γ^* Dependence on the Interlayer Distance for a Constant Magnetic Field.

Chapter 5

Magnetic Instabilities in a Superlattice

5.1 The Single Quantum Well Superlattice

The absence of a stable SDW phase in a single quantum well can be understood as a consequence of the independence of the Coulomb interaction matrix element of the $2D$ momentum $\vec{k}$, as demonstrated in Ch. 3. This result implies that by adding an additional degree of freedom to the electron motion, such that the interaction depends on the electron momentum, a stable SDW can be realized. Searching for SDW phases in double quantum well systems (DWQS) or superlattices (SL) is based on the intuition that the motion of the electrons in a direction perpendicular to the layers, within a periodic potential established during the growth process of the semiconductor structure, modifies the energy spectrum and enhances the many-body interactions conducing to a more favorable situation for the creation of spin instabilities.

In this chapter we discuss the possible existence of a stable SDW state in a type-I superlattice, generically described as a sequence of N ($N \to \infty$) identi-

cal, infinitely attractive quantum wells of strength $-\lambda$ (of zero width, essentially 2D planes) displaced along the $\hat{z}$-axis at equal intervals a. The periodic potential established along the SL axis is

$$V(z) = -\lambda \sum_l \delta(z - la) \; . \tag{5.1}$$

In this picture, each well of potential $V_0(z) = -\lambda\delta(z)$ has just one bound electron state, described by state function

$$\nu(z) = \sqrt{\kappa} e^{-\kappa|z|} \; , \tag{5.2}$$

and energy

$$\epsilon_0 = -\frac{\hbar^2\kappa^2}{2m} \; , \tag{5.3}$$

where $\kappa = m\lambda/\hbar^2$.

A magnetic field is applied under an angle with the superlattice axis, such that the cyclotron energy and the Zeeman splitting of the electron levels become comparable. Weak tunneling is allowed between the wells along the z direction, with tunneling probability $e^{-\kappa a} \ll 1$. The single electron wave function in the superlattice is a product of the usual 2D wave function that describes the quantized Landau levels inside each well ($x-y$ motion), Eq. (3.6) and a $\hat{z}$-dependent wave function, $\zeta(z)$ which is the solution of a Schrödinger equation written for the SL potential,

$$\left[-\frac{\hbar^2}{2m}\frac{d^2}{dz^2} - \lambda \sum_l \delta(z - la) \right] \zeta(z) = \epsilon\zeta(z) \; . \tag{5.4}$$

The lowest energy state can be obtained by a variational principle in the tight binding approximation, when a solution $\zeta(z)$ is written as a linear combination of localized

wave functions multiplied by a periodic phase factor. This strategy implies that the electron momentum along the $\hat{z}$ direction is a valid quantum number. When periodic boundary conditions are assumed, k_z is given by $\frac{2\pi}{Na}j$ ($j = -N/2, N/2$). Within this approximation, ζ_{k_z} is written

$$\zeta_{k_z}(z) = \frac{1}{\sqrt{N}} \sum_l e^{ik_z la} \nu(z - la) \; . \tag{5.5}$$

Up to first order in the tunneling probability, the norm of $\zeta_{k_z}(z)$ is

$$\langle \zeta_{k_z} | \zeta_{k_z} \rangle = 1 + 2e^{-\kappa a} \cos k_z a \; . \tag{5.6}$$

The energy E_{k_z} is obtained immediately as the average of the Hamiltonian on the state ζ_{k_z},

$$E_{k_z} = \frac{< \zeta_{k_z} | \frac{p^2}{2m} + V(z) | \zeta_{k_z} >}{< \zeta_{k_z} | \zeta_{k_z} >} \; , \tag{5.7}$$

The numerator is calculated by noticing that $\frac{p^2}{2m} + V_0(z - na)$ represents the Hamiltonian of the well located at $z = na$. Hence, if we denote by $\delta V(z - na)$ the potential difference,

$$\delta V(z - na) = V(z) - V_0(z - na) = -\lambda \sum_{l \neq 0} \delta(z - na - la) \; , \tag{5.8}$$

Eq. (5.7) becomes:

$$E_{k_z} = \frac{< \zeta_{k_z} | \frac{p^2}{2m} + V_0(z - na) + \delta V(z - na) | \zeta_{k_z} >}{< \zeta_{k_z} | \zeta_k >} \; , \tag{5.9}$$

leading to

$$E_k \simeq \epsilon_0 + \frac{1}{N}\sum_{l,m} e^{ik_z(m-l)a} < \nu(z-la)|\delta V(z-ma)|\nu(z-ma) > \ . \tag{5.10}$$

It is clear, therefore, that as a result of the tunneling, the single energy level of a quantum well is broadened into a miniband, whose infinitesimally close energy levels are given, up to first order in the tunneling probability by:

$$E_k = \epsilon_0 \left[1 + 4e^{-\kappa a}\cos(\kappa a)\right] \ . \tag{5.11}$$

We introduce the width of the miniband, Δ as the difference between the maximum and minimum energies:

$$\Delta = -8\epsilon_0 e^{-\kappa a} \ . \tag{5.12}$$

Eqs. (5.5) and (5.11) are consequently used to write the total state function and energy of an electron in the three dimensional space. The relevant quantum numbers are n, the Landau level index, k_y, k_z and σ. Hence,

$$\Psi_{n,k_y,k_z,\sigma}(x,y,z) = \zeta(z)\psi_{n,k_y,\sigma}(x,y) \ , \tag{5.13}$$

where $\psi_{n,k_y}(x,y)$ is the $2D$ wave function, expressed in Eq. (3.6). The energy of this single electron state is

$$\epsilon_{n,k_z,\sigma} = \hbar\omega_c\left(n+\frac{1}{2}\right) + \gamma\sigma B - \frac{\Delta}{2}(1 + 4e^{-\kappa a}\cos k_z a) \ . \tag{5.14}$$

5.2 The Many-Body Picture of the Spin Density Wave Instability

As suggested by our analysis of spin instabilities in a single quantum well, the existence of a spin-density wave phase is possible if the system can be brought into a state that favors the simultaneous formation of triplet excitons from a paramagnetic or a ferromagnetic ground state. Moreover, the fundamental premise of the SDW formation, namely a collective pairing of opposite spin states that differ by the same momentum $\vec{Q}$, in this case, $|k_z, \uparrow>$ and $|k_z + Q_z, \downarrow>$, should be realized. We refer here only to the momentum k_z along the $\hat{z}$ axis, since the in-plane momentum does not play any role in the SDW coupling.

First, we reevaluate the energy involved in the many-body driven spin-flip excitations that occur between the minibands $|0, k_z, \uparrow>$ and $|1, k_z, \downarrow>$. In this analysis, the momentum k_z is restricted to the first Brillouin zone, defined by the interval $(-\pi/a, \pi/a)$.

Starting from a paramagnetic configuration, where for all k_z, $|0, k_z, \uparrow>$ is lower than $|1, k_z, \downarrow>$, as described in Fig. 5.1, the most energetically advantageous transition corresponds to an electron from the edge of the first Brillouin zone of $|0, k_z, \uparrow>$ moving to the center of the Brillouin zone of $|1, \downarrow>$. This indicates that the coupling wave vector for the resulting electron-hole pair is equal to $Q_z = \frac{\pi}{a}$, which corresponds to the shortest wave vector in the $\epsilon(\kappa)$ vs. k_z diagram that would be compatible with this indirect transition. If we adopt $Q_z = \frac{\pi}{a}$ as the common coupling wave vector of all the triplet excitons that are created, it is easier to pursue our analysis by displacing the $|1, k_z, \downarrow>$ miniband by this amount in the momentum space and study the spin flip transitions between $|0, k_z, \uparrow>$ and $|1, k_z + Q_z, \downarrow>$.

The overlapping of these two minibands starts at the edge of the Brillouin

zone, at $k_z = -\frac{\pi}{a}$. A triplet exciton is formed when an electron from $|0, -\frac{\pi}{a}, \uparrow\rangle$ jumps on $|1, 0, \downarrow\rangle$, leaving a hole of opposite spin behind. Its energy is equal to:

$$W = \epsilon - \Delta + \epsilon^x_{01} - \epsilon^x_{00} + \gamma^x_{01} \ , \tag{5.15}$$

where ϵ and ϵ^x_{nm}'s have the same significance as in the case of the single quantum well. For a quick numerical evaluation of W, in the simplest approximation, we consider that all energies in Eq. (5.15) have the same values as in 2D, defined by Eqs. (3.22), (3.23) and (3.24), with the exception of Δ, Eq. (5.12), which is determined by the inter-layer tunneling. By choosing $|\epsilon^x_{00}|$ as the energy unit, we arrive at the condition that defines the stability of the triplet exciton, i.e., $W < 0$, which requires

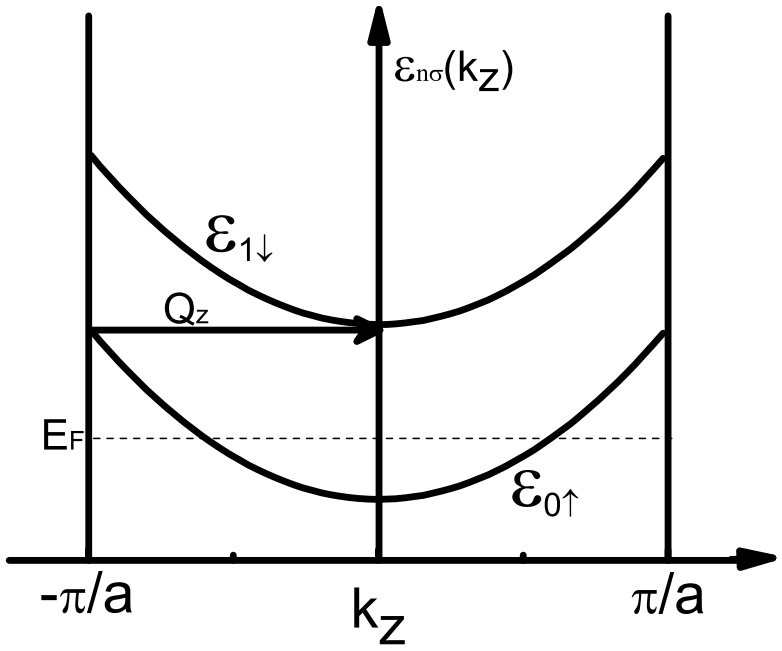

Figure 5.1: The Formation of a Triple Exciton from the Paramagnetic State in a Single Quantum Well

ϵ to satisfy:

$$\epsilon < 0.073 + \Delta \ . \tag{5.16}$$

Similarly, at the center of the Brillouin zone, the spin-flip transition of an electron from $|1, 0, \downarrow\rangle$ onto $|0, \frac{\pi}{a}, \uparrow\rangle$ leads to the formation of a triplet exciton of energy:

$$W' = -\epsilon - \Delta - \epsilon^x_{11} - \epsilon^x_{10} + \gamma^x_{01} \ . \tag{5.17}$$

The stability condition $W' < 0$ generates a second bound on ϵ:

$$\epsilon > 0.667 - \Delta \ . \tag{5.18}$$

Eqs. (5.16) and (5.18) define the area of the phase transition in the energy-tunneling plane. The SDW formation is possible for values of the bandwidth larger than the critical value defined by the intersection of the two lines, $\Delta_c = 0.37|\epsilon^x_{00}|$. This defines the area of the common solutions for the simultaneous stability of the triplet excitons that form in a paramagnetic or ferromagnetic ground state. In essence this is the result obtained in Ref. [33].

As Fig. 5.2 shows, the nature of the ground state depends critically on the magnitude of the bandwidth Δ. At small bandwidth Δ, the system undergoes a paramagnetic to ferromagnetic transition, essentially behaving like a 2D system. For values of Δ exceeding a critical value Δ_c a SDW ground state becomes possible. In between, both paramagnetic and ferromagnetic phases are stable and the SDW state is an unstable HF solution.

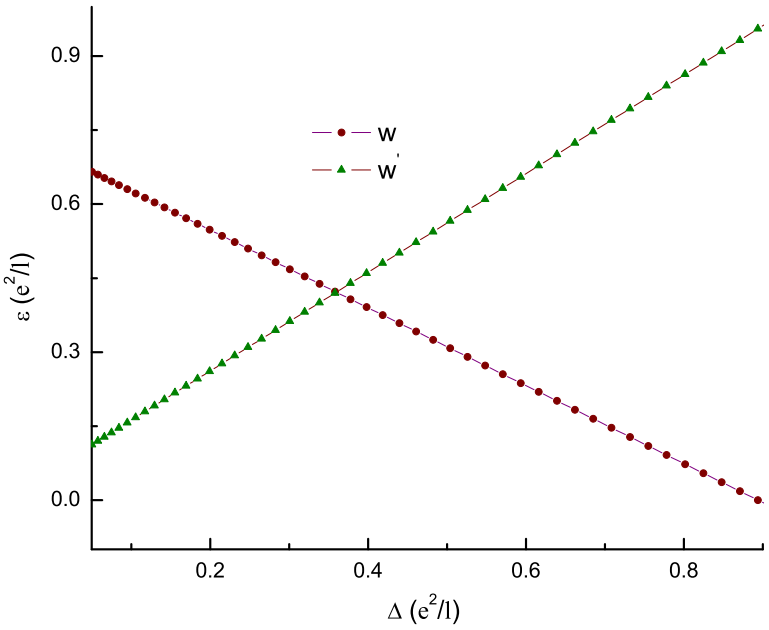

Figure 5.2: The Energy Curves of the Triple Excitons Formed in the Paramagnetic and Ferromagnetic States of a Single Quantum Well

5.3 A Many-Body Picture of the SDW Phase

A complete calculation of a possible SDW state, however, requires the input provided by the Coulomb interaction among the electrons. The Coulomb interaction matrix element that describes the coupling of two electrons in states $|n, k_z, k_y, \sigma >$ and $|m, k_z + Q_z, k_y + Q_y, \sigma' >$ which exchange momentum $\vec{q}$ is

$$v_{nm}(k_z, q, Q) = \int d\vec{r_1} \int d\vec{r_2} \psi^*_{n,k+Q}(\vec{r_1}) \psi^*_{m,k+q}(\vec{r_2}) \frac{e^2}{|\vec{r_1} - \vec{r_2}|} \psi_{m,k}(\vec{r_2}) \psi_{n,k+Q}(\vec{r_1}) \ . \quad (5.19)$$

The computational effort necessary for the evaluation of Eq. (5.19) is greatly reduced by performing the Fourier transform of the bare Coulomb potential, such that $\frac{e^2}{|\vec{r_1} - \vec{r_2}|} \longrightarrow \sum_{\vec{q}} \frac{4\pi e^2}{q^2} e^{i\vec{q}\cdot(\vec{r_1} - \vec{r_2})}$. Then,

$$v_{nm}(k, q, Q) = \int d\vec{r_1} \int d\vec{r_2} \psi^*_{n,k+Q}(\vec{r_1}) \psi^*_{m,k+q}(\vec{r_2}) \sum_q \frac{4\pi e^2}{q^2} e^{i\vec{q}\cdot(\vec{r_1} - \vec{r_2})} \psi_{m,k}(\vec{r_2}) \psi_{n,k+Q}(\vec{r_1}) \ . \quad (5.20)$$

When the expressions for the state functions, Eq. (5.13), are inserted, the integral along the $\hat{z}$ axis separates and we can write,

$$v_{nm}(k_z, Q_z, q_z, Q_y, q_y) = \frac{2e^2}{\pi} F(k_z, Q_z, q_z) \int_{-\infty}^{\infty} dq_{0x} \frac{e^{-\frac{l^2}{2}(q_y^2 + 2iq_{0x}Q_y + q_{0x}^2)}}{q_{0x}^2 + q_y^2} w_{nm}\left(\frac{q_{0x}^2 + q_y^2}{2} l^2\right) \ , \quad (5.21)$$

where w_{nm} is given by Eq. (3.17). The form factor $F(k_z, Q_z, q_z)$ is determined by the Coulomb interaction mediated superposition of the one-electron wave functions in the $\hat{z}$-direction:

$$F(k_z, q_z, Q_z) = \int_{-\infty}^{\infty} dz_1 \int_{-\infty}^{\infty} dz_2 \zeta^*_{k_z}(z_1) \zeta^*_{k_z + Q_z + q_z}(z_2) e^{iq_z(z_2 - z_1)} \zeta_{k_z + Q_z}(z_2) \zeta_{k_z + q_z}(z_1) \ . \quad (5.22)$$

By making use of Eq. (5.5), after a lengthy, but otherwise straightforward calculation, we obtain:

$$\begin{aligned} F(k_z, q_z, Q_z) &= 1 + 4e^{-\kappa a} \cos\frac{Q_z a}{2} \left[\left(\cos\frac{q_z a}{2} + \frac{2\kappa}{q_z} \sin\frac{q_z a}{2} \right) \cos\left(k_z + \frac{Q_z + q_z}{2} \right) a \right. \\ &- \left. (1 + \kappa a) \cos\left(k_z + \frac{Q_z}{2} \right) a \right] . \end{aligned} \tag{5.23}$$

All the functions $\zeta(z)$ are considered normalized.

In the spin-flip transitions analyzed above, the electrons on the lowest miniband $|0, k_z, \downarrow>$ play a passive role, limited to providing some exchange interaction with the electrons on $|1, k_z, \downarrow>$. For simplicity, the miniband is assumed to be fully occupied and remains such even when a SDW state is being established. Its occupancy is determined by $N \times N_L$, where N_L is the degeneracy of a Landau level for a given intensity of the applied magnetic field.

To describe the electron states in the active minibands, we introduce the creation and destruction operators $c^\dagger_{0,k_z,\uparrow}, c_{0,k_z,\uparrow}$ for the electrons in $|0, k_z, \uparrow>$ and $c^\dagger_{1,k_z,\downarrow}, c_{1,k_z,\downarrow}$ for the electrons in $|1, k_z, \downarrow>$. In the absence of the interaction, the equilibrium Hamiltonian is H_0 given by

$$\begin{aligned} H_0 &= N_L \sum_{k_z} \left(\frac{1}{2}\hbar\omega_c - \hbar\omega_s + \frac{\Delta}{2}\cos k_z a \right) + \sum_k \left(\frac{1}{2}\hbar\omega_c + \hbar\omega_s + \frac{\Delta}{2}\cos k_z a \right) c^\dagger_{0k_z\uparrow} c_{0k_z\uparrow} \\ &+ \sum_{k_z} \left(\frac{3}{2}\hbar\omega_c - \hbar\omega_s + \frac{\Delta}{2}\cos k_z a \right) c^\dagger_{1k_z\downarrow} c_{1k_z\downarrow} . \end{aligned} \tag{5.24}$$

When the Coulomb interaction is considered, the relevant terms reflect the coupling between all the electron states involved:

$$H_{int} = -\frac{1}{2} \sum_{k,q,Q,\sigma,\sigma'} v_{nm}(k, q, Q) c^\dagger_{n,k+q+Q,\sigma} c^\dagger_{m,k,\sigma'} c_{m,k+q,\sigma'} c_{n,k+Q,\sigma} . \tag{5.25}$$

The ground state energy of the system, which is the average of the total Hamiltonian on the ground state wave function, cannot be obtained unless certain approximations are performed on the interaction terms. As discussed in Ch.2, in the Hartree-Fock approximation, the ground-state average of the product of four operators is factorized into a product of two two-particle operators, according to Eq. (2.5). For now, no assumption is made on the nature of the ground state. Thus, with $< \ldots, \ldots >$ representing the ground state average, the interaction becomes,

$$\begin{aligned} H_{int} = & -\frac{1}{2} \sum_{k_z,q_z,Q_z,\sigma,\sigma'} v_{nm}(k_z,q_z,Q_z) < c^{\dagger}_{n,k_z+q_z+Q_z,\sigma} c_{n,k_z+Q_z,\sigma} >< c^{\dagger}_{m,k_z,\sigma'} c_{m,k_z+q_z,\sigma'} > \\ - & \frac{1}{2} \sum_{k_z,q_z,Q_z,\sigma,\sigma'} v_{nm}(k_z,q_z,Q_z) < c^{\dagger}_{n,k_z+q_z+Q_z,\sigma} c_{m,k_z+q_z,\sigma'} >< c^{\dagger}_{m,k_z,\sigma'} c_{n,k_z+Q_z,\sigma} > \end{aligned} \tag{5.26}$$

The first term of Eq. (5.26) represents the direct interaction, $< c^{\dagger}_{n,k_z+q_z+Q_z,\sigma} c_{n,k_z+Q_z,\sigma} >= \delta_{q_z,0}$, which is canceled out by the positive background. The second term generates the exchange and the SDW potentials:

$$\begin{aligned} & < c^{\dagger}_{n,k_z+q_z+Q_z,\sigma} c^{\dagger}_{m,k_z,\sigma'} c_{m,k_z+q_z,\sigma'} c_{n,k_z+Q_z,\sigma} > \\ = & < c^{\dagger}_{n,k_z+q_z,\sigma} c_{m,k_z+q_z,\sigma} >< c^{\dagger}_{m,k_z,\sigma} c_{n,k_z,\sigma} > \delta_{Q_z,0} \delta_{\sigma,\sigma'} \\ - & < c^{+}_{n,k_z+q_z+Q_z,\sigma} c_{m,k_z+q_z,\sigma'} >< c^{\dagger}_{m,k_z,\sigma'} c_{n,k_z+Q_z,\sigma} > \delta_{\sigma,\sigma'} \ . \end{aligned} \tag{5.27}$$

We finally write,

$$\begin{aligned} H_{int} = & -\frac{1}{2} \sum_{k_z,q_z,\sigma} v_{nm}(k_z,q_z,0) < c^{\dagger}_{n,k_z+q_z,\sigma} c_{m,k_z+q_z,\sigma} >< c^{\dagger}_{m,k_z,\sigma} c_{n,k_z,\sigma} > \delta_{Q_z,0} \delta_{\sigma,\sigma'} \\ - & \frac{1}{2} \sum_{k_z,q_z,Q_z} v_{nm}(k_z,q_z,Q_Z) < c^{\dagger}_{n,k_z+q_z+Q_z,\sigma} c_{m,k_z+q_z,\sigma'} >< c^{\dagger}_{m,k_z,\sigma'} c_{n,k_z+Q_z,\sigma} > \end{aligned} \tag{5.28}$$

By explicitly declaring all the terms the interaction, we obtain:

$$
\begin{aligned}
H_{int} = & -\sum_{k_z,q_z} v_{00}(k_z,q_z,0) < c^{\dagger}_{0,k_z+q_z,\downarrow} c_{0,k_z+q_z,\downarrow} >< c^{\dagger}_{0,k_z,\downarrow} c_{0,k_z,\downarrow} > \\
- & \sum_{k_z,q_z} v_{00}(k_z,q_z,0) < c^{\dagger}_{0,k_z+q_z,\uparrow} c_{0,k_z+q_z,\uparrow} >< c^{\dagger}_{0,k_z,\uparrow} c_{0,k_z,\uparrow} > \\
- & \sum_{k_z,q_z} v_{10}(k_z,q_z,0)[< c^{\dagger}_{0,k_z+q_z,\downarrow} c_{0,k_z+q_z,\downarrow} > c^{\dagger}_{1,k_z,\downarrow} c_{1,k_z,\downarrow} + < c^{\dagger}_{0,k_z,\downarrow} c_{0,k_z,\downarrow} > c^{\dagger}_{1,k_z+q_z,\downarrow} c_{1,k_z+q_z,\downarrow} \\
- & \sum_{k_z,q_z} v_{11}(k_z,q_z,0) < c^{\dagger}_{1,k_z+q_z,\downarrow} c_{1,k_z+q_z,\downarrow} >< c^{\dagger}_{1,k_z,\downarrow} c_{1,k_z,\downarrow} > \\
- & \frac{1}{2} \sum_{k_z,q_z,Q_Z} v_{10}(k_z,q_z,Q_z) \Big[< c^{+}_{0,k_z+q_z+Q_z,\uparrow} c_{1,k_z+q_z,\downarrow} >< c^{+}_{1,k_z,\downarrow} c_{0,k_z+Q_Z,\uparrow} > \\
+ & < c^{+}_{1,k_z+q_z+Q_z,\downarrow} c_{0,k_z+q_z,\uparrow} >< c^{+}_{0,k_z,\uparrow} c_{1,k_z+q_z+Q_Z,\downarrow} > \Big] \ . \qquad (5.29)
\end{aligned}
$$

The terms of the interaction Hamiltonian that appear in Eq. (5.29) are the exchange energy of the electrons in the $|0,k_z,\downarrow>$ level, the exchange energy of the electrons on $|1,k_z\ \downarrow>$ interacting with those on the $|0,k_z,\downarrow>$ level, followed by the exchange of the $|0,k_z,\uparrow>$ particles, of the $|1,k_z,\downarrow>$ particles among themselves, and finally the interaction of the electrons on $|0,k_z,\uparrow>$ and those on $|1,k_z,\downarrow>$. The latter term is present only if one assumes that operator averages of the type $< c^{\dagger}_{0k\uparrow} c_{1k+Q\downarrow} > \neq 0$. This is clearly not the case if one considers the usual electron distribution inside the Fermi sphere. But, if one envisions a state in which the average is different from zero, that state would describe a collective pairing of electrons of opposite spins and momenta k_z and $k_z + Q_z$. This is the fundamental premise of the SDW formation.

To understand the microscopic structure of an average of the type $< c^{\dagger}_{0k_z\uparrow} c_{1k_z+Q_z\downarrow} >$, a canonical Bogoliubov-Valatin (BV) transformation is performed. This introduces two new operators α_{k_z} and β_{k_z} defined as :

$$
\begin{aligned}
c_{0k_z\uparrow} &= \cos\theta_{k_z}\alpha_{k_z} + \sin\theta_{k_z}\beta_{k_z} \ , \\
c_{1k_z+Q_z\downarrow} &= -\sin\theta_{k_z}\alpha_{k_z} + \cos\theta_{k_z}\beta_{k_z} \ . \qquad (5.30)
\end{aligned}
$$

where the angle θ_{k_z} is the variational parameter of the transformation. Substituting the electron operators by the Eqs. (5.30), leads to an expression for the ground state energy that depends on averages of the newly introduced operators, α_{k_z} and β_{k_z}. There are four types of terms that appear. Two represent the same particle averages, $< \alpha^{\dagger}_{k_z}\alpha_{k_z} >$ and $< \beta^{\dagger}_{k_z}\beta_{k_z} >$, and two mixed-ones, $< \alpha^{\dagger}_{k_z}\beta_{k_z} >$ and $< \beta^{\dagger}_{k_z}\beta_{k_z} >$. The first category can be easily associated with the occupation numbers of two new quasiparticles, while the second is clearly describing the excitation processes of these quasiparticles. Since the ground state of the system is of interest, we will neglect the quasiparticle excitations. Thus, by the means of the BV transformation, the system of interacting electrons is transformed into a system of non-interacting quasiparticles. It is worth pointing out that the structure of the canonical transformation is similar to that of Eqs. (2.18) and (2.20) that describe the SDW waves in the electron gas.

As a function of the quasiparticle occupation numbers, $f_{1k_z} =< \alpha^{\dagger}_{k_z}\alpha_{k_z} >$ and $f_{2k_z} =< \beta^{\dagger}_{k_z}\beta_{k_z} >$,the ground state energy becomes,

$$
\begin{aligned}
&\langle H\rangle_{HF} = N_L \sum_{k_z}\left(\frac{1}{2}\hbar\omega_c - 2\gamma B + \frac{\Delta}{2}\cos k_z a\right)\\
+\;& \sum_{k_z}\left(\frac{1}{2}\hbar\omega_c + 2\gamma B - \frac{\Delta}{2}\cos k_z a\right)\left(\cos^2\theta_{k_z} f_{1k_z} + \sin^2\theta_{k_z} f_{2k_z}\right)\\
+\;& \sum_{k_z}\left[\frac{3}{2}\hbar\omega_c - 2\gamma B - \frac{\Delta}{2}\cos(k_z+Q_z)a\right]\left(\sin^2\theta_k f_{1k_z} + \cos^2\theta_{k_z} f_{2k_z}\right)\\
-\;& \frac{1}{2}\sum_{k_z,k_z{}'} v_{00}(k_z, k_z^{'} - k_z, 0)\left(\cos\theta^2_{k_z} f_{1k_z} + \sin^2\theta_{k_z} f_{2k_z}\right)\left(\cos\theta^2_{k_z'} f_{1k_z'} + \sin^2\theta_{k_z'} f_{2k_z'}\right)\\
-\;& \frac{1}{2}\sum_{k_z,k_z{}'} v_{11}(k_z+Q_z, k_z^{'} - k_z, 0)\left(\sin^2\theta_{k_z} f_{1k_z} + \cos^2\theta_{k_z} f_{2k_z}\right)\left(\sin^2\theta_{k_z'} f_{1k_z'} + \cos^2\theta_{k_z'} f_{2k_z'}\right)\\
-\;& \sum_{k_z,k_z'} v_{10}(k_z, k_z' - k_z, 0)\left(\sin^2\theta_{k_z} f_{1k_z} + \cos^2\theta_{k_z} f_{2k_z}\right)\\
-\;& \frac{1}{4}\sum_{k_z,k_z{}'} v_{10}(k_z, k_z^{'} - k_z, Q_z)\sin 2\theta_{k_z}\sin 2\theta_{k_z'}(f_{1k_z} - f_{2k_z})(f_{1k_z'} - f_{2k_z'})\;, \qquad (5.31)
\end{aligned}
$$

where we introduced $q_z = k'_z - k_z$. Eq. (5.31) is quite general and can be used to describe the system at all temperatures. Here, we will focus only on obtaining the lowest energy of the system at $T = 0K$. Hence, we consider only the lowest energy quasiparticle to exist and consequently set $f_{1k_z} = 1$, while $f_{2k_z} = 0$. Under these circumstances, a minimum of $\langle H \rangle_{HF}$ as the function of θ_{k_z} is reached when $\partial \langle H \rangle_{HF} / \partial \theta_{k_z} = 0$. This condition generates the self-consistent SDW equation,

$$\begin{aligned} & \sin(2\theta_k) \left[\frac{3}{2}\hbar\omega_c - 2\gamma B - \frac{\Delta}{2}\cos(k_z + Q_z)a - \sum_{k'_z} v_{11}(k_z + Q_z, k'_z - k_z, 0) \sin^2\theta_{k'_z} \right. \\ - & \sum_{k'_z} v_{10}(k_z + Q_z, k'_z - k_z, 0) \\ - & \left. \frac{1}{2}\hbar\omega_c + 2\gamma B - \frac{\Delta}{2}\cos k_z a + \sum_{k'_z} v_{00}(k_z, k'_z - k_z, 0) \cos^2\theta_{k'_z} \right] \\ = & \cos(2\theta_k) \sum_{k'_z} v_{10}(k_z, k'_z - k_z, Q_z) \sin 2\theta_{k'_z} \ . \end{aligned} \tag{5.32}$$

We introduce the single particle energies in the HF approximation,

$$\tilde{\epsilon}_{0,k_z,\uparrow} = \frac{1}{2}\hbar\omega_c + \gamma B - \frac{\Delta}{2}\cos k_z a - \sum_{k'_z} v_{00}(k_z, k'_z - k_z, 0) \cos\theta^2_{k'_z} \ , \tag{5.33}$$

for the electrons in the $|0, k_z, \uparrow>$ miniband and

$$\begin{aligned} \tilde{\epsilon}_{0,k_z+Q_z,\downarrow} &= \frac{3}{2}\hbar\omega_c - \gamma B - \frac{\Delta}{2}\cos(k_z + Q_z)a \\ - & \sum_{k'_z} v_{11}(k_z + Q_z, k'_z - k_z, 0) \sin^2\theta_{k'_z} - \sum_{k'_z} v_{10}(k_z + Q_z, k'_z - k_z, 0) \ , \end{aligned} \tag{5.34}$$

for the electrons in the $|1, k_z + Q_z, \downarrow>$ miniband, and write the inclination angle equation in its consecrated form,

$$\tan(2\theta_{k_z}) = \frac{g(k_z)}{\tilde{\epsilon}_{1,k_z+Q_{z,\downarrow}} - \tilde{\epsilon}_{0,k_{z,\uparrow}}} \ , \tag{5.35}$$

where we define the SDW gap to be

$$g_{k_z} = \sum_{k'_z} v_{10}(k_z, k'_z - k_z, Q_z) \sin 2\theta_{k'_z} \ . \tag{5.36}$$

Eq. (5.35) is a non-local, self-consistent expression, since the solution is dependent on the values of the inclination angle throughout the Brillouin zone. g_{k_z} is called the SDW gap since it represents the difference between the energy of the two quasiparticle states that exist in the SDW phase, as one can see by differentiating Eq. (5.31) with respect to the corresponding occupation numbers, f_{1k_z} and f_{2k_z} respectively:

$$E_{1,2}(k_z) = \frac{1}{2}\left[\tilde{\epsilon}_{1,k_z+Q_z,\downarrow} + \tilde{\epsilon}_{0,k_z,\uparrow} \mp \sqrt{(\tilde{\epsilon}_{1,k_z+Q_z,\downarrow} - \tilde{\epsilon}_{0,k_z,\uparrow})^2 + g_{k_z}^2}\right] \ . \tag{5.37}$$

When the single-particle energies, written in the HF approximation, in the opposite spin minibands become degenerate, $\tilde{\epsilon}_{1,k_z+Q_z,\downarrow} = \tilde{\epsilon}_{0,k_z,\uparrow}$, the two quasiparticle energies differ by g_{k_z}.

The stability condition for the SDW phase is $\partial^2 < H >_{HF} / \partial\theta_{k_z}^2 < 0$, which is always realized when a solution to the gap equation is found since,

$$\frac{\partial^2 < H >_{HF}}{\partial\theta_{k_z}^2} = -\sqrt{(\tilde{\epsilon}_{1,k_z+Q_z,\downarrow} - \tilde{\epsilon}_{0,k_z,\uparrow})^2 + g_{k_z}^2} \ . \tag{5.38}$$

An analytic solution for Eq. (5.35) is not possible and one needs to resort to a numerical algorithm, a challenging task given the non-local self-consistency of the problem. The starting point of the calculation is the replacement of the discrete sums by integrals over k_z. When the expression of the Coulomb interaction is considered from Eq. (5.21) along with Eq. (5.23), we write, after several simple manipulations,

for the gap function,

$$g_{k_z} = \frac{e^2}{l}\int_{-\infty}^{\infty} d\xi F(k_z, \xi/l - k_z, Q_z)\sin 2\theta(\xi)\int_0^{\infty} dx \frac{e^{-\frac{x^2}{2}}}{x^2 + (\xi - k_z l)^2}\left(1 - \frac{x^2}{2}\right) J_0(lQ_y x) \tag{5.39}$$

while for the energies in the denominator we obtain,

$$\begin{aligned}
\tilde{\epsilon}_{1,k_z+Q_z,\downarrow} &= \frac{3}{2}\hbar\omega_c - 2\gamma B - \frac{\Delta}{2}\cos(k_z + Q_z)a \\
- &\frac{e^2}{l}\int_{-\infty}^{\infty} d\xi F(k_z + Q_z, \xi/l - k_z, 0)\sin^2\theta(\xi)\int_0^{\infty} dx \frac{e^{-\frac{x^2}{2}}}{x^2 + (\xi - k_z l)^2}\left(1 - \frac{x^2}{2}\right)^2 \\
- &\frac{e^2}{l}\int_{-\infty}^{\infty} d\xi F(k_z + Q_z, \xi/l - k_z, 0)\int_0^{\infty} dx \frac{e^{-\frac{x^2}{2}}}{x^2 + (\xi - k_z l)^2}\left(1 - \frac{x^2}{2}\right) ,
\end{aligned} \tag{5.40}$$

and

$$\begin{aligned}
\tilde{\epsilon}_{0,k_z,\uparrow} &= \frac{1}{2}\hbar\omega + \gamma B - \frac{\Delta}{2}\cos(k_z + Q_z)a \\
- &\frac{e^2}{l}\int_{-\infty}^{\infty} d\xi F(k_z, \xi/l - k_z, 0)\cos^2\theta(\xi)\int_0^{\infty} dx \frac{e^{-\frac{x^2}{2}}}{x^2 + (\xi - k_z l)^2} .
\end{aligned} \tag{5.41}$$

A quick inspection of these equations suggests that an appropriate numerical algorithm for solving Eq. (5.35) is based on an iterative method, where an initial input solution is used to calculate the right hand side. Then, the new values for the inclination angle, calculated from the gap equation, are considered the input values in a new iteration. The detailed computational program is presented in Appendix A. The iteration proceeds until the convergence of the solution.

We note that the 2D limit of the gap equation, obtained when there is no interlayer tunneling, does not admit a solution. It is therefore necessary that one chooses an apriori value for the free parameters of the problem. The most important is the coupling vector Q_z chosen here to be π/a, consistent with the situation depicted

in Fig. (5.1). Then, the difference in the kinetic energies, $\epsilon - \Delta$, is chosen in agreement with Fig. (5.2), where a minimum value for Δ is specified. Moreover, we choose $Q_y l = 1.2$, the value that maximizes the exciton binding energy in 2D. The parameters that enter the gap equation are, therefore, the gap width, Δ, the tunneling probability $e^{-\kappa a}$ and the ratio of the superlattice constant and the magnetic length $\frac{a}{l}$.

The dependence of the solution of the gap equation on these parameters is shown below. In Fig. 5.3, we present the results of our numerical algorithm showing the influence of the superlattice constant on the inclination angle, for a given magnetic field. In units of $|\epsilon^x_{00}|$, we chose $\epsilon = 0.5$ and $\epsilon_0 = 0.9$ in Eq. (5.12). As a/l increases, the inclination angle of the SDW is increasing toward the edges of the Brillouin zone, while the overall curve narrows toward the center. This behavior suggests that as the distance between the wells increases, the superlattice properties are replaced by a single quantum well behavior, which for the given parameters is most probably ferromagnetic.

Increasing the inter-well tunneling probability, for the same superlattice constant, leads to an increase of the polarization angle, an expected consequence of the increased band overlap, as well as of the enhanced electron-electron interaction. These results are shown in Fig. 5.4.

The quasiparticle energy in the ground state is presented in Fig. 5.5. The spin polarization, which is proportional to $\cos 2\theta_{k_z}$ is presented in Fig. 5.6.

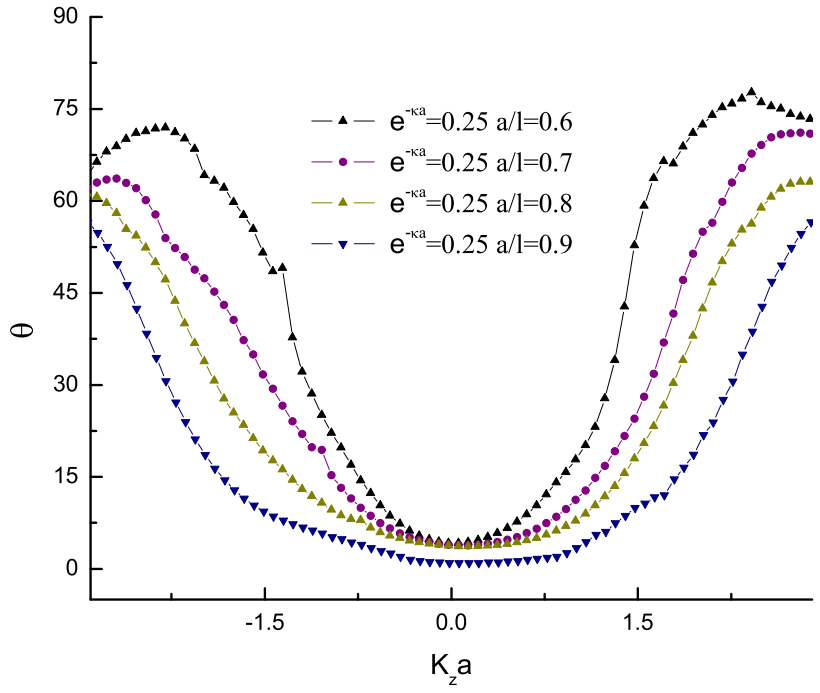

Figure 5.3: SDW Polarization Angle in First Brillouin Zone of a Single Well Superlattice

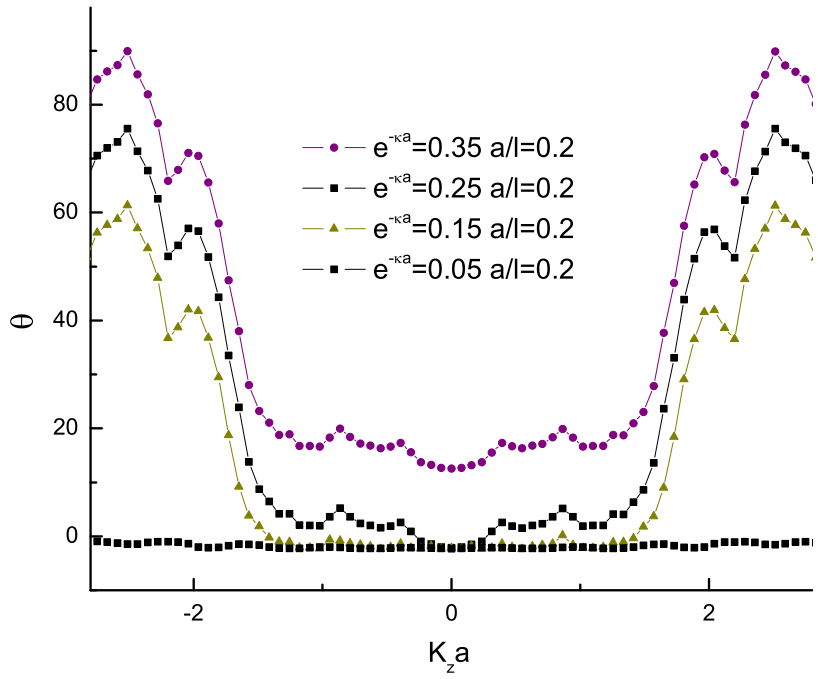

Figure 5.4: Inclination Angle in First Brillouin Zone Studied as a Function of a/l For Different Tunneling Probabilities

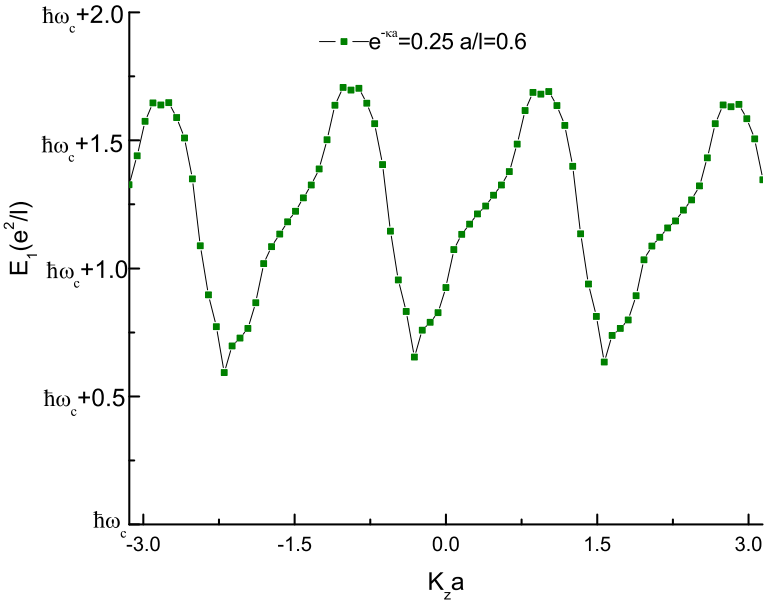

Figure 5.5: The Energy Spectrum of the Low Energy Excitation in the SDW State.

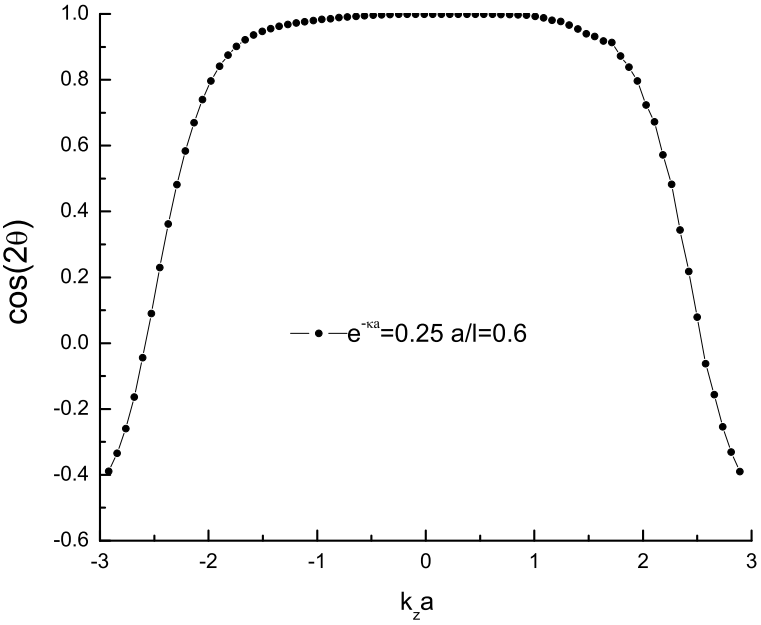

Figure 5.6: The Spin Polarization in the SDW Phase

Chapter 6

Spin Density Waves In the Lowest Landau Level Of a Superlattice in a Tilted Magnetic Field

6.1 The Double Quantum Well Superlattice

In double quantum well systems, whose layers are coupled by tunneling, in the presence of a tilted magnetic field, the new energy scale introduced by the symmetric/antisymmetric splitting competes with the Zeeman interaction and the Landau level spacing and can be used as an additional parameter that, in certain conditions favors a spin mode softening, or equivalently spin-flip transitions. This result was first derived by Zheng et. al [34] and refined in a series of subsequent papers by Das Sarma et al. [35], [15]. In each case, the manipulation of the energy levels by adjusting the polarizing magnetic field or the tunneling was conducive to a miniband alignment which could be overcome by the many-body interaction, leading to the formation of a ground state of the electron system with a canted antiferromagnet configuration

[36]. This can be explained by the enlargement of the phase space that introduces more available states for the electron scattering, whereby enhancing the effect of the interaction. By varying the tunneling probability and the spatial separation between the two wells, the interplay among the inter-well and intra-well electron correlations can be investigated. In fact, the competition among the Coulomb interaction energy, the spin splitting, Landau spacing and the symmetric-antisymmetric splitting caused by interlayer tunneling determines the magnetic nature of the ground state.

In this chapter we extend the analysis of the spin instabilities to the case of a superlattice whose unit cell is a double layer system. This structure combines the attributes of a double quantum well system with the modulated periodicity of the electronic wave function along the superlattice axis. As we will demonstrate below, its complex energy band alignment permits the investigation of spin-flip transitions within the same Landau level, leading to the establishment of stable SDW phases. The technological advantage of such a system consists in eliminating the large scale energy of the problem, the cyclotron energy, in favor of two relatively small energies, the Zeeman splitting and Δ_{SAS}. The typical SL system appropriate for this application is a type I, GaAs-based structure, such that the electrons are confined within GaAs.

In a simple model for the double-quantum-well-superlattice (DQWSL), we consider the wells in each unit cell to be infinitely attractive, of strength $-\lambda$ and separated by a distance $2a$. The cell is periodically repeated N times along the $\hat{z}$ axis, with period b, where $b > 2a$. The potential experienced by an electron is a superposition of all the localized attractive potentials:

$$V(z) = -\lambda \sum_{l} [\delta(z + a + lb) + \delta(z - a + lb)] \; . \tag{6.1}$$

The single particle state function can be built within the tight binding approximation

as a superposition of localized wave functions modulated by periodic amplitudes:

$$\zeta_\alpha(k_z, z) = \frac{1}{\sqrt{N}} \sum_l e^{ik_z lb} \nu_\alpha(z - lb) \ , \tag{6.2}$$

where $\nu_\alpha(z)$ is the DQWS wave function given in Eq. (4.9) with α being the symmetric (S) or antisymmetric (A) index. Eq. (6.2) explicitly introduces the electron momentum along the $\hat{z}$ direction as a good quantum number, which on account of periodic boundary conditions assumes a quasicontinuum $k_z = \frac{2\pi}{Nb} j$ ($j = -\frac{N}{2}, \frac{N}{2}$). Since there are two linear independent states for an electron in the unit cell, in the superlattice two distinct minibands are generated, labeled by the same indices. The $x - y$ motion is described by Eq. (3.6), independent of the $\hat{z}$ degree of freedom.

The single particle Hamiltonian for the motion along the superlattice axis is

$$H = \frac{p^2}{2m} - \lambda[\delta(z - lb - a) + \delta(z - lb + a)] + \delta V \tag{6.3}$$

where δV represents the non-local potential, with respect to the well located at $z = b$,

$$\delta V = -\lambda \sum_{l' \neq l} [\delta(z - l'b - a) + \delta(z - l'b + a)] \ . \tag{6.4}$$

We calculate the single particle energy within the tight binding approximation, exactly as described in the preceding chapter. Hereby, we estimate

$$\begin{aligned} E_{\alpha,k_z} &= < \zeta_{\alpha,k_z} | H | \zeta_{\alpha,k_z} > \\ &= \langle \zeta_{\alpha,k_z} | \frac{p^2}{2m} - \lambda\delta(z - lb - a) - \lambda\delta(z - lb + a) + \delta V | \zeta_{\alpha,k_z} \rangle \\ &= \epsilon_{k_z} - \frac{\lambda}{N} \sum_{n \neq l} \sum_{l,m} e^{i\kappa(l-m)b} \left[\langle \nu_{\alpha,k_z}(z - mb) | \delta(z - nb - a) | \nu_{\alpha,k_z}(z - lb) \rangle \right. \\ &+ \left. \langle \nu_{\alpha,k_z}(z - mb) | \delta(z - nb + a) | \nu_{\alpha,k_z}(z - lb) \rangle \right] \ . \end{aligned} \tag{6.5}$$

In a first order approximation, we consider only tunneling between adjacent wells, such that $l - m = \pm 1$. Moreover, we assume that $b < 4a$, such that tunneling between two different superlattice cells occurs only between the wells separated by a distance equal to $b - 2a$. With this,

$$E^{A}_{S,k_z} = \epsilon_0 \Big[1 \mp (\lambda\kappa) 2 \cos(k_z b) e^{-\kappa(b-2a)} (1 \pm e^{-2\kappa a}) \Big] \,, \tag{6.6}$$

where ϵ_0 is the bound state energy in a single quantum well, Eq. (5.3). This result describes the broadening of the two sublevels of a single DQWS cell into two minibands in the superlattice, with the upper sign being associated with the antisymmetric level, while the lower corresponds to the symmetric level.

To calculate the Coulomb interaction between the electrons in this superlattice, we consider three-dimensional electron states. These are described by the tensor product between the 2D wave functions, Eq. (3.6), and the one along the third direction, Eq. (6.2),

$$\Psi_{\alpha,n,k_z,k_y,\sigma} = \zeta_{\alpha,k_z}(z) \psi_{n,k_y,\sigma}(x,y) \,. \tag{6.7}$$

Since in the following analysis we discuss only spin-flip transitions within the lowest Landau level, the $n = 0$ Landau level index is no longer explicitly declared.

The energy of a spin-flip transition is given by the difference between the energy of the electron after and before the event. To obtain this result, we start by calculating the matrix element that describes the scattering of two electrons between the initial states $\{|\alpha, k_z + q_z, k_y + q_y, \sigma >, |\beta, k_z + Q_z, k_y + Q_y, \sigma' >\}$ into the final states $\{|\alpha, k_z, k_y, \sigma >, |\beta, k_z + Q_z + q_z, k_y + Q_y + q_y, \sigma' >\}$,

$$v_{\alpha\beta}(\vec{k}, \vec{Q}, \vec{q}) = \int d\vec{r_1} \int d\vec{r_2} \psi^{*}_{\alpha,\vec{k}+\vec{Q}+\vec{q}}(\vec{r_1}) \psi^{*}_{\beta,\vec{k}}(\vec{r_2}) \frac{e^2}{|\vec{r_1} - \vec{r_2}|} \psi_{\beta,\vec{k}+\vec{q}}(\vec{r_2}) \psi_{\alpha,\vec{k}+\vec{Q}}(\vec{r_1}) \,. \tag{6.8}$$

As before, the calculation is greatly simplified if the Coulomb interaction is replaced by its 3D Fourier series, $e^2/r \longrightarrow \sum_{\vec{q_0}} 4\pi e^2/q_0^2$.

Based on the two dimensional system calculation [11], as well as that on the first type of superlattice [33], we can write directly

$$v_{\alpha\beta}(k_z, q_y, q_z, Q_y, Q_z) = F_{\alpha\beta}(k_z, q_z, Q_z) \int_{-\infty}^{\infty} dq_{0x} \frac{1}{q_y^2 + q_{0x}^2 + q_z^2} e^{-\frac{l^2}{2}(q_y^2 + 2iq_{0x}Q_y + q_{0x}^2)} , \tag{6.9}$$

where $F_{\alpha\beta}(k_z, q_z, Q_z)$ are the form factors that describe the Coulomb interaction mediated superposition of the electron states along the $\hat{z}$ axis.

The associated interaction energies are obtained by summing over all the possible value of the exchanged momentum, $\{q_y, q_z\}$. Hence, for the electrons in the lowest Landau level, we write

$$\epsilon_{\alpha\beta}(\vec{k}, \vec{Q}) = \frac{e^2}{l} \int_{\infty}^{\infty} d\xi F_{\alpha\beta}^*(\xi, k_z) F_{\alpha\beta}(\xi, k_z + Q_z) \int_0^{\infty} dx \frac{x e^{-\frac{x^2}{2}}}{x^2 + \xi^2} J_0(x, lQ_y) , \tag{6.10}$$

The three different types of form factors possible involve coupling between electrons inside each of the minibands or between electrons inside different minibands. In the Hartree-Fock approximation adopted here, the exchange energies result when $Q_y = 0, Q_z = 0$, whereas the electron-binding energy is calculated at a finite Q_y, Q_z. The specific form factors are,

$$\begin{aligned} & F_{SS}(k_z, q_z, 0) = \cos q_z a \left\{ \cos q_z a + 2e^{-2\kappa a} \left[\rho(q_z a) - 1 \right] \right. \\ + \quad & \left. 4e^{-2\kappa(b-2a)} \left\{ \rho \left[q_z \left(b - \frac{a}{2} \right) \right] \cos \left(k_z + \frac{q_z}{2} \right) b - \rho(0) \cos k_z b \right\} \right\} , \end{aligned} \tag{6.11}$$

for the $S-S$ exchange,

$$\begin{aligned} & F_{AA}(k_z,q_z,0)=\cos q_z a\left\{\cos q_z a-2e^{-2\kappa a}\rho(q_z a)\right. \\ - \quad & \left. e^{-2\kappa(b-2a)}\left\{\rho\left[q_z\left(b-\frac{a}{2}\right)\right]\cos\left(k_z+\frac{q_z}{2}\right)b-\rho(0)\cos k_z b\right\}\right\}\ , \end{aligned} \tag{6.12}$$

for the $A-A$ exchange and finally, for the $A-S$ exchange,

$$F_{AS}(k_z,q_z,0)=\cos q_z a\left\{\cos q_z a+2e^{-2\kappa(b-2a)}\left\{\rho\left[q_z\left(b-\frac{a}{2}\right)\right]\sin\left(k_z+\frac{q_z}{2}\right)b-\rho(0)\sin k_z b\right\}\right\}\ , \tag{6.13}$$

where,

$$\rho(x)=\cos x+2\kappa a\frac{\sin x}{x}\ . \tag{6.14}$$

In turn, the electron-hole binding energy is mediated by a form factor calculated at finite Q_z,

$$\begin{aligned} & F_{AS}(k_z,q_z,Q_z)=\sin q_z a\left\{\sin q_z a+2e^{-2\kappa(b-2a)}\cos\left(\frac{Q_z b}{2}\right)\right. \\ & \left.\times\left\{\rho\left[q_z\left(b-\frac{a}{2}\right)\right]\sin\left(k_z+\frac{q_z}{2}+\frac{Q_z}{2}\right)b-\rho(0)\sin k_z b\right\}\right\}\ . \end{aligned} \tag{6.15}$$

The analysis of the excitonic instabilities that can occur in this system is a necessary stepping stone in finding a favorable situation for the formation of a stable SDW state.

When $\Delta_{SAS}<2\gamma B$, the lowest occupied minibands are $|0,S,\downarrow>$ and $|0,A,\downarrow>$, defining a ferromagnetic ground state, as depicted in Fig. (4.2). The spin-flip transition from $|0,A,\downarrow>$ onto $|S,\uparrow\rangle$, starts when an electron from the edge of the Brillouin zone of the down-spin miniband, jumps to the lowest energy point in the up-spin miniband, which corresponds to a finite coupling wavevector $Q_z=\pi/b$. The energy

of the triplet exciton thus formed is

$$W = \epsilon - \epsilon^x_{A\downarrow A\downarrow} - \epsilon^x_{A\downarrow S\downarrow} + \gamma_{S\uparrow A\downarrow} \ , \tag{6.16}$$

an expression that counts the lost exchange $\epsilon^x_{A\downarrow A\downarrow}$ and $\epsilon_{A\downarrow S\downarrow}$ and binding energy $\gamma_{S\uparrow A\downarrow}$.

Similarly, at the center of the Brillouin zone, the overlap of the minibands of interest occurs when the electron on $|A, 0, \downarrow\rangle$ jumps onto $|S, \frac{\pi}{b}, \uparrow\rangle$, which corresponds to a paramagnetic initial state described in Fig. (4.1), when $2\gamma B < \Delta_{SAS}$. The energy associated with the formation of the triplet exciton is now:

$$W' = -\epsilon - \epsilon^x_{S\uparrow S\uparrow} + \epsilon^x_{A\downarrow S\downarrow} + \gamma_{S\uparrow A\downarrow} \ , \tag{6.17}$$

where we include the lost exchange with the electrons on the same S miniband as well as with those on the S miniband and the gained binding energy.

By plotting W and W' as a function of the tunneling probability, we define the region in the phase space where the two excitons can be simultaneously formed. A quick estimate is obtained by considering the effect of the tunneling only on the kinetic energies of the electrons, a result showed in Fig. (6.1).

Compared with the case of a single quantum well superlattice, the different behavior of the DQWSL arises from the intra-unit cell tunneling, which allows for possible spin instabilities even in the absence of an inter-unit cell contribution. This is region where the canted antiferromagnetic state, described in Ref. [34] occurs. Our result shows that when the inter-unit cell tunneling appears, the canted antiferromangetic phase extends to the whole superlattice, forming, on account of periodicity, a SDW.

6.2 The Spin Density Wave Phase

We discuss the formation of a SDW ground state within the Hartree-Fock approximation by assuming that the $|S, k_z, \downarrow>$ and $|A, k_z, \downarrow>$ minibands are fully occupied. The former miniband does not participate in the dynamics of the system, beyond providing some exchange interaction with the same spin electrons in the active minibands, $|S, k_z, \uparrow>$ and $|A, k_z, \downarrow>$.

Inspired by the results developed in Ch.5, we associate the existence of a SDW with a finite value for $< c^{\dagger}_{Ak_z\downarrow} c_{Sk_z+Q_z\uparrow} >$, when the average is performed on the ground state. Consequently, we introduce the canonical transformation

$$\begin{aligned} c_{Sk_z\uparrow} &= \cos\theta_{k_z}\alpha_{k_z} + \sin\theta_{k_z}\beta_{k_z} \\ c_{Ak_z+Q_z\downarrow} &= -\sin\theta_{k_z}\alpha_{k_z} + \cos\theta_{k_z}\beta_{k_z} \end{aligned} \tag{6.18}$$

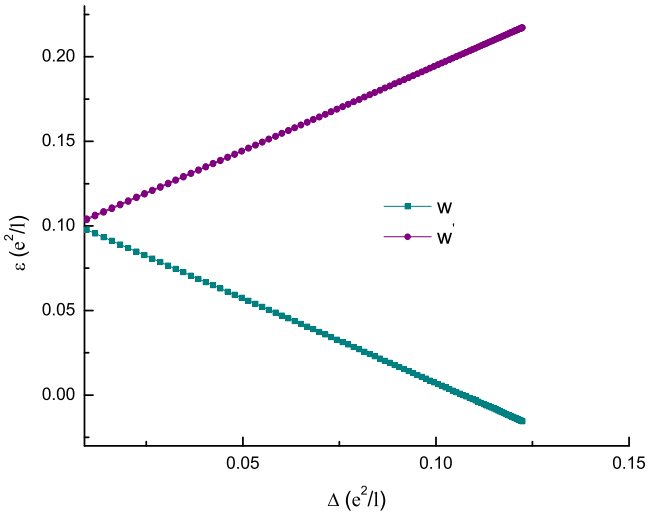

Figure 6.1: The Magnetic Phase Diagram of a Double Quantum Well Superlattice

that describes the two branches of the SDW, with θ_{k_z} the variational parameter. The diagonal form of the total energy of the system, written in terms of the new operators α_{k_z} and β_{k_z} becomes,

$$
\begin{aligned}
H_{HF} &= \sum_{k_z} \epsilon_{Sk_z\downarrow} - \frac{1}{2}\sum_{k_z,q_z} v_{S\downarrow S\downarrow}(k_z,q_z,0) + \sum_{k_z} \epsilon_{Sk_z\uparrow}\Big[\cos^2\theta_{k_z} f_{1k_z} + \sin^2\theta_{k_z} f_{2k_z}\Big] \\
- & \frac{1}{2}\sum_{k_z,k'_z} v_{S\uparrow S\uparrow}(k_z,k'_z-k_z,0)(\cos^2\theta_{k_z} f_{1k_z} + \sin^2\theta_{k_z} f_{2k_z})\left(\cos^2\theta_{k'_z} f_{1k'_z} + \sin^2\theta_{k'_z} f_{2k'_z}\right) \\
+ & \sum_{k_z} \epsilon_{Ak_z+Q_z\downarrow}\left(\sin^2\theta_{k_z} f_{1k_z} + \cos^2\theta_{k_z} f_{2k_z}\right) \\
- & \frac{1}{2}\sum_{k_z,k'_z} v_{A\downarrow A\downarrow}(k_z,k'_z-k_z,0)\left(\sin^2\theta_{k_z} f_{1k_z} + \cos^2\theta_{k_z} f_{2k_z}\right)(\sin^2\theta_{k'_z} f_{1k'_z} + \cos^2\theta_{k'_z} f_{2k'_z}) \\
- & \sum_{k_z,k'_z} v_{A\downarrow S\downarrow}(k_z,k'_z-k_z,0)\left(\sin^2\theta_{k_z} f_{1k_z} + \cos^2\theta_{k_z} f_{2k_z}\right) \\
- & \frac{1}{4}\sum_{k_z,k'_z} v_{A\uparrow S\downarrow}(k_z,k'_z,Q)\sin 2\theta_{k_z}(f_{1k_z}-f_{2k_z})\sin\theta_{k'_z}(f_{1k'_z}-f_{2k'_z})\ .
\end{aligned}
\tag{6.19}
$$

$\epsilon_{\alpha,k_z,\sigma}$ are the kinetic energies,

$$
\epsilon_{\alpha,k_z,\sigma} = \frac{\hbar\omega_c}{2} + \sigma\gamma B + E_{\alpha,k_z}\ , \tag{6.20}
$$

with E_{α,k_z} given by Eq. (6.6), and $f_{1k_z} =< \alpha^\dagger_{k_z}\alpha_{k_z} >$ and $f_{2k_z} =< \beta^\dagger_{k_z}\beta_{k_z} >$ the occupation numbers of the two SDW quasiparticles.

Obtaining the minimum energy, from $\partial < H >_{HF} /\partial\theta_{k_z}$ leads to a self-consistent gap equation,

$$
\tan[2\theta(k_z)] = \frac{g(k_z)}{\tilde{\epsilon}_{S,k_z+Q_{z,\downarrow}} - \tilde{\epsilon}_{S,k_{z,\uparrow}}}\ , \tag{6.21}
$$

where $\tilde{\epsilon}_{0,k_{z,\uparrow}}$ and $\tilde{\epsilon}_{1,k_z+Q_{z,\downarrow}}$ are the Hartree-Fock energies of the particles involved in

the SDW coupling,

$$\begin{aligned}
\tilde{\epsilon}_{S,k_z,\uparrow} &= \frac{1}{2}\hbar\omega_c + \gamma B + E_{S,k_z} - \sum_{k'_z} v_{S\uparrow S\uparrow}(k_z, k'_z - k_z, 0)\cos\theta^2_{k'_z} \ , \\
\tilde{\epsilon}_{A,k_z+Q_z,\downarrow} &= \frac{1}{2}\hbar\omega_c - \gamma B + E_{A,k_z+Q_z} - \sum_{k'_z} v_{A\downarrow A\downarrow}(k_z + Q_z, k'_z - k_z, 0)\sin^2\theta_{k'_z} \\
&- \sum_{k'_z} v_{S\downarrow A\downarrow}(k_z + Q_z, k'_z - k_z, 0) \ , \qquad (6.22)
\end{aligned}$$

respectively. The gap function g_{k_z} is represented by

$$g_{k_z} = \sum_{k'_z} v_{A\downarrow S\uparrow}(k_z, k'_z - k_z, Q_z)\sin 2\theta_{k'_z} \ . \qquad (6.23)$$

Eq.(6.21) is solved by an iterative method, self-consistently, for each value of k_z within the first Brillouin zone $\left(-\frac{\pi}{b}, \frac{\pi}{b}\right)$, as a function of the tunneling probability. The SDW pairing vector is taken to be $Q_z = \pi/b$. A typical solution obtained for an inter-cell tunneling probability $e^{-\kappa(b-2a)} = 0.35$, $a/l = 0.2$ and $b/l = 0.8$ is presented in Fig. (6.2).

We remark on the existence of a finite inclination angle in the center of the Brillouin zone, whose origin can be traced back to the canted antiferromagnetic ground state of a DQWS. The two symmetric peaks are the remnants of the ferromagnetic coupling at the edge of the Brillouin zone of the DQWS, now strongly diminished by the interference effects present in the superlattice.

The variation of the SDW angle with the intra-unit cell separation between the wells is described in Fig. (6.3). For several chosen parameters, defined by the inter-unit cell tunneling probability $e^{-\kappa(b-2a)} = 0.25$, $b/l = 0.8$, we calculate the polarization angle when a/l assumes different values. As the distance between the wells composing the unit cell increases, an interesting regular pattern, described by a sequence of almost equally spaced peaks is established. This can be understood by

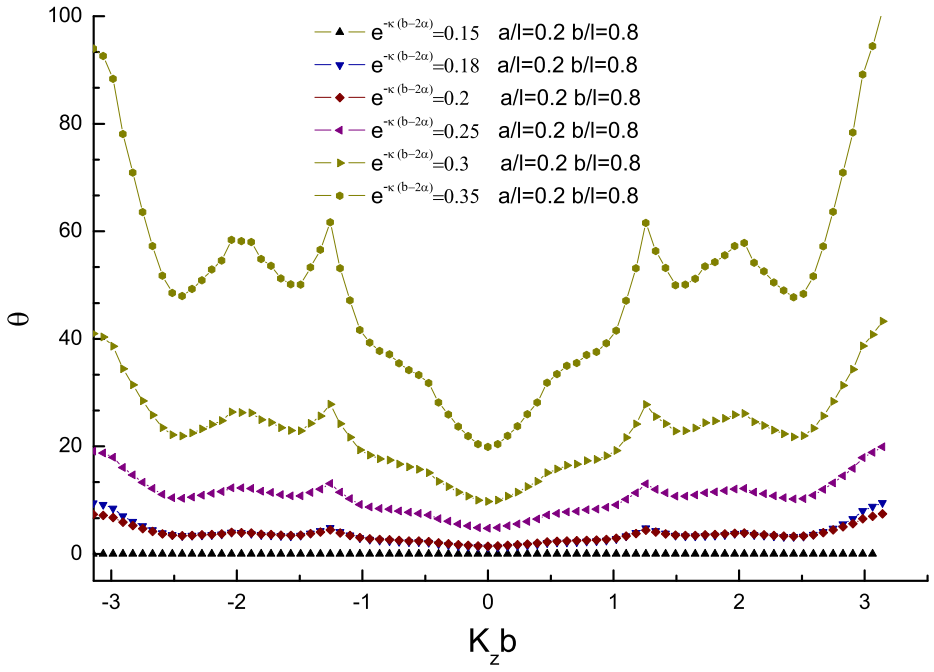

Figure 6.2: Polarization Direction of a SDW in a Double-Quantum Well System Plotted as a Function of the Tunneling Probability for a Fixed SL Constant

noticing that as the wells get separated they recover the single quantum well properties, and an incipient paramagnetic to ferromagnetic transition appears. Therefore, the peaks can be seen as the signature of the ferromagnetic orientation at the edge of the Brillouin zone of a single well, modulated by the inter-well tunneling and the SL periodicity.

The effect of the inter-cell tunneling on the inclination angle is presented in Fig. 6.4. For the same values of the inter-well tunneling probability and the intra-unit cell distance between the wells, we calculate the polarization angle as a function of the DQWSL constant, b/l. As b/l increases, the SL properties are being replaced by the DQWS characteristics, leading to a smooth variation of the angle. For low b/l, the interference effects between the unit cells aligned along the superlattice axis

generate the periodic pattern of peaks discussed before.

In Fig. 6.5 we compare the polarization angle of a SDW in a single quantum well superlattice with the polarization angle of a SDW in a double quantum well superlattice for the same value of the inter-unit cell tunneling and for the same intra-unit cell distance between the wells (in the case of the single well system this is the SL constant). In the end we present the results for the spin polarization, which is proportional to $\cos 2\theta_{k_z}$ in Fig. (6.6).

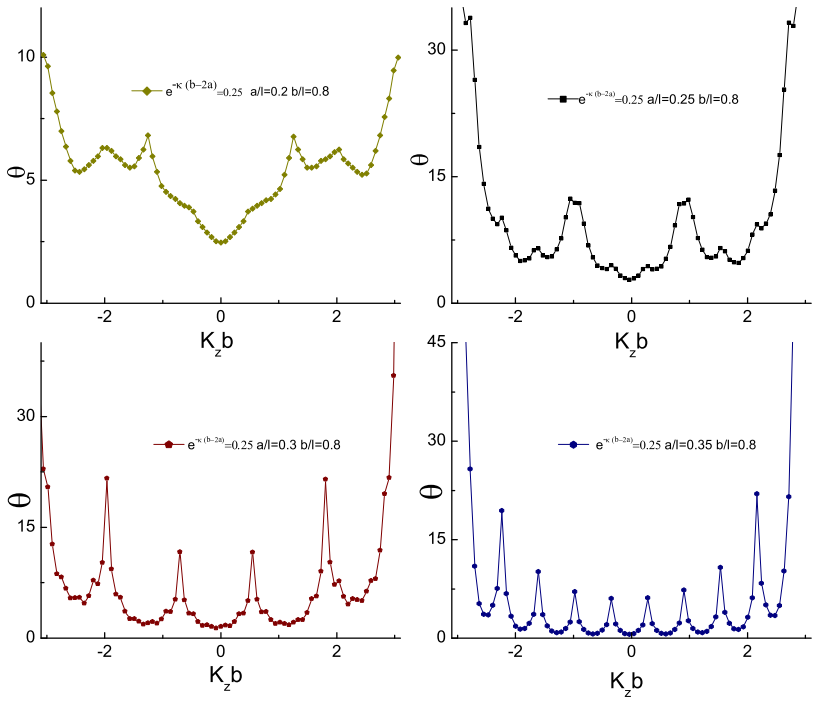

Figure 6.3: Variation of the SDW Angle With the Intra-unit Cell Tunneling

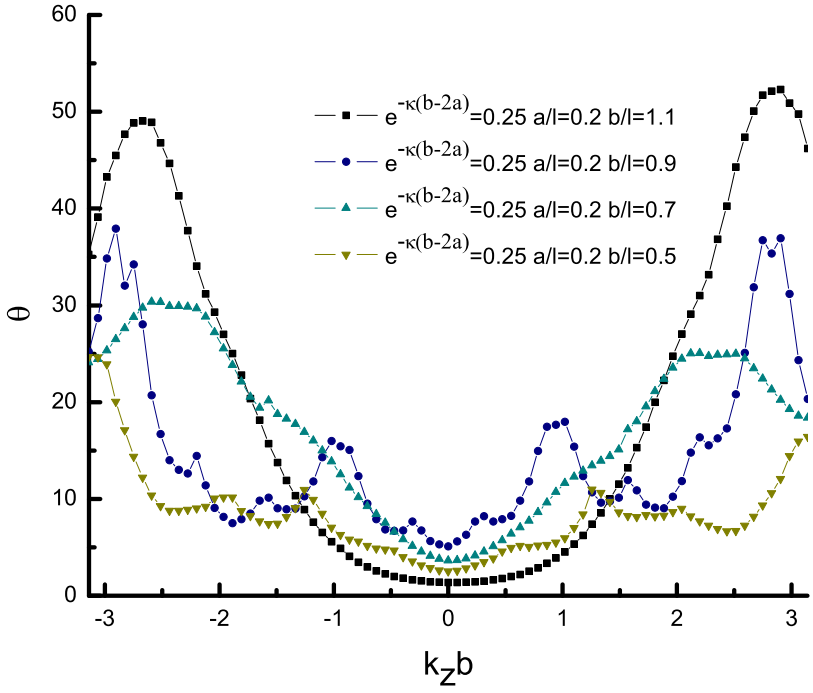

Figure 6.4: Variation of the SDW Angle With the Inter-unit Cell Tunneling

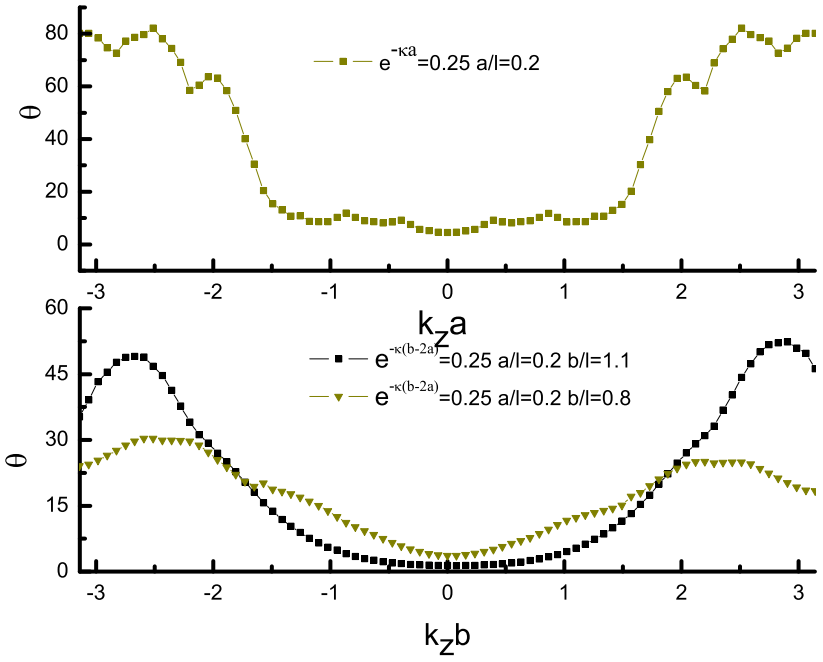

Figure 6.5: Comparison of the SDW Polarization Angle in a Single and Double Quantum Well Superlattice

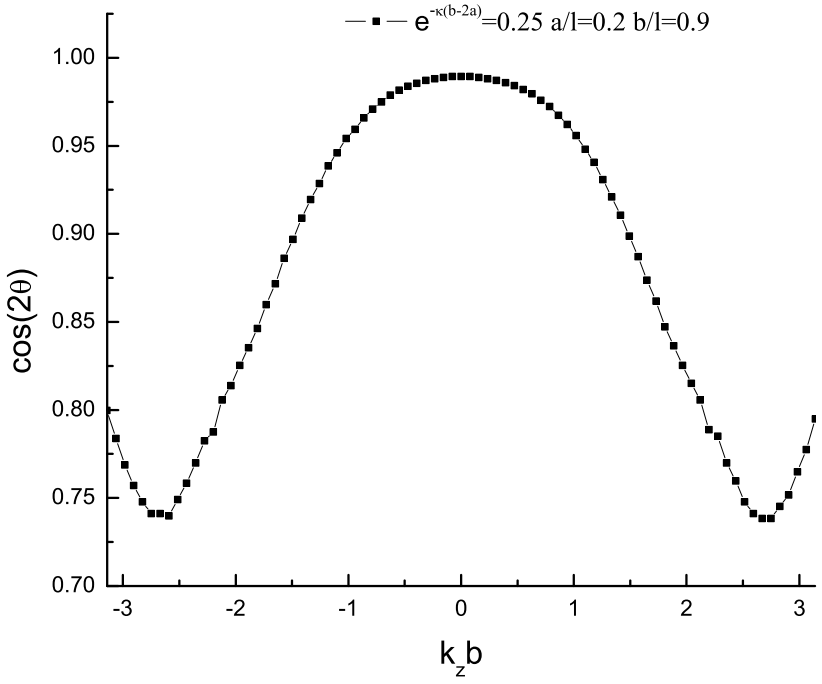

Figure 6.6: Spin Polarization in the SDW Phase of a Double Quantum Well Superlattice

Chapter 7

Conclusions

Realizing stable SDW phases in semiconductor superlattices at low temperature is a consequence, mostly, of a perfectly controlled energy band alignment that leads to a spin degeneracy. On this basis, a long range off-diagonal order of the electrons of opposite spins and momenta differing by the same value $\vec{Q}$ can occur. Our numerical estimates indicate that such a broken spin symmetry phase can be realized under specific, but experimentally realizable, circumstances. In this sense, this is a driven transition, since it is conditioned by the presence of a magnetic field, and not spontaneous as in the Overhauser model of the SDW states in the electron gas. Nonetheless, the experimental observation of this one-dimensional SDW can greatly enrich our understanding of the many-body interaction in the electron systems. In the case of the DQW-SL system the influence of the magnetic field is minimized because only two relatively small energies, the Zeeman splitting and the symmetric-antisymmetric splitting are involved.

The main constraint that conditions the applicability of the models discussed in this paper refers to the density of the electrons in the system that has to be high enough to assure that the first two Landau levels/minibands are occupied. This

justifies the validity of the Hartree-Fock approximation, on which our calculation is based. Departures from this scenario are not trivial, because they involve electron correlations, the dynamic effects that relate to the short range Coulomb repulsion. According to many authors, however, it is exactly the correlation effects that destroy the long range off-diagonal order that characterizes the SDW phase. Thus, studying the formation of SDW in systems whose electron density can be varied, such as semiconductor SL, offers the extremely interesting opportunity of producing a convincing experimental measure of this argument.

From a different perspective, the controlled realization of a modulated spin polarization in a semiconductor structure, offers the potential applicability of this system to various spintronics applications (where "spintronics" refers to anything related to "spin based electronics".) For this to happen, more detailed studies are needed, most importantly, the effect of temperature. Our calculation, done at very low temperature, considers just the low lying SDW quasiparticles, whereas at a higher temperature, both excitations, along with their distribution functions, calculated self-consistently, have to be taken into account. Moreover, at some critical temperatures, the thermal fluctuations will destroy the spin order regardless of the external fields that favor the alignment, and the system will transition to the normal, paramagnetic state. More detailed calculations are necessary for a complete understanding of the problem.

Appendices

Appendix A Self-Consistent Solution to the SDW Gap Equation for the Single Well Superlattice

```
#include "stdafx.h"
#include"stdio.h"
#include"math.h"
#include "stdafx.h"
#include <vector>

using namespace std ;

const double pi = 3.14159265 ;

struct Z{
      double z ;
      double theta;
      Z(double z,double theta)
         {
         this->z = z ;
         this->theta = theta ;
         }
       } ;

double v(int k,double kza,double t, double d, vector<Z>& arr_z );
double w(int k,double y);
double vv(int k, double lQy, double kza, double d, double x1);
double  c(double z,double kza,double t,double Qza ,double d);
double BESJ0(double x) ;

void main( )
{
      double t, d, kza, delta, eps, deps;
      double d0, v0, v1, v2, g;

 //-------------------------------------------------------

      double step1  ;
      double theta ;
      int i, j, l, nmax, nmax2, nmax4;

 //-------------------------------------------------------

      t =4;
      d = 0.3f;
      nmax=80;
      eps = 0.5*sqrt(pi/2.0);
      delta =0.9*sqrt(pi/2.0);
      kza= -pi;
      step1=2*pi/nmax;
      nmax4 = 6;

      double* kzaarr = new double[nmax+1];
      double* thetaarr = new double[nmax+1];

 //-------------------------------------------------------

 for(j=0; j <= nmax ;j++)
      {
            kzaarr[j] = kza ;
            thetaarr[j] = kza/2 ;
            kza = kza + step1;
      }

      if(remove( "zq4.txt" ) == -1 )

      {
        perror( "Could not delete 'ZQ4.TXT'" );
      }

      else
      {
        printf( "Deleted 'zq4.txt'\n" );
      }
```

```
      FILE *fp4;

      if ((fp4=fopen("zq4.txt","a+"))==NULL)
      {
        printf("cannot open this file\n");
        return    ;
      }

      fprintf(fp4,"kza theta e1 e2\n");
      printf("kza theta e1 e2\n");

      //-------------------------------------------------

      // this step initializes the file theta.txt

      //-------------------------------------------------

      for(i = 1 ; i<=nmax4 ; i++)
      {
         fprintf(fp4,"%i iterator \n" , i);
         printf("%i iterator \n" , i);
         nmax2 = -9 ;
         vector<Z> arr_z ;

         for( l = 1; l<= 2*abs(-9)+1 ;l++)
            {
               for(j=0; j <= nmax ;j++)
                  {
                   kza = kzaarr[j] ;
                   theta=thetaarr[j] ;
                   double z = 2*pi*nmax2 + kza ;
                   arr_z.push_back(Z(z,theta));
                  }
                  nmax2 = nmax2+ 1  ;
            }

            //-----------------------------------------------------

            // at each iteration, the program reads the current
            // values of kza and theta; this step initializes
            //   the file z.txt

            //-----------------------------------------------------

         for(j=0; j <= nmax ; j++)
            {
              kza = kzaarr[j] ;
              d0 = eps + delta*cos(kza) ;
              v0 = v(0,kza,t,d,arr_z) ;
              v1 = v(1,kza,t,d,arr_z) ;
              v2 = v(2,kza,t,d,arr_z);
              deps = d0-v1-v2+v0 ;
              g = v(3,kza,t,d,arr_z) ;

              if(g/deps >= 0)
                {
                 theta = 0.5*atan(g/deps) ;
                 }
              else
                {
                 theta = pi/2-0.5*atan(-g/deps);
                 }

              double e2 = -v2-v1+sqrt(pow(deps ,2) + pow(g ,2)) ;
              double e1= -v0-sqrt(pow(deps ,2) + pow(g,2)) ;

              fprintf(fp4,"%f,  %f,  %f,  %f \n", kza, theta, e1, e2);
              printf("%f %f %f %f  \n", kza, theta, e1, e2);
              thetaarr[j] = theta ;
              }
      }

      fclose(fp4);

      printf( "Press RETURN to finish:" );
      char c = getchar();
}


//-----------------------------------------------------------------

double v(int k, double kza, double t, double d, vector<Z>& arr_z )
 {
      int  i,nmax1, nmax2 ;
      double del1  ;
      double sum1, z ;
```

```
      nmax1 = 81 ;
      nmax2 = 7*nmax1;
      del1 = 2*pi/nmax1;
      sum1 = 0.0;
      int  count = arr_z.size() ;

 for(i=0; i<count; i++)
   {
       double z = arr_z[i].z ;
       double theta = arr_z[i].theta ;

   switch(k)
    {
   case 0:
     sum1 = sum1+c(z*d-kza,kza,t,0.0,d)*w(k,z-kza/d)*pow(cos(theta),2);
     break ;
   case 1:
     sum1 = sum1+w(k,z-(kza+pi)/d)*c(z*d-(kza+pi),kza+pi,t,0.0,d);
     break;
   case 2:
     sum1 = sum1+c(z*d-(kza+pi),kza+pi,t,0.0,d)*w(k,z-(kza+pi)/d)*pow(sin(theta),2);
     break;
   case 3:
     sum1 = sum1+c(z*d-kza,kza,t,pi,d)* w(k,z-kza/d)*sin(2*theta);
     break;
        }
    }

   return sum1*del1/pi;
}


//-------------------------------------------------

double w(int k, double y)
{
      double  x, b ;
      int nmax ;
      double sum2, del2 ;

      b = 1.2f ;
   // b=1.2 is the value of Q_yl which realizes the instability in 2D.
      sum2 = 0.0 ;
      nmax = 500 ;
      del2 = 50.0/nmax ;
      x = del2/2 ;

      for(int j = 0; j < nmax + 1 ; j++)
      {
        switch(k)
         {
          case 0:
            sum2 = sum2 + x*exp(-x*x/2)/(x*x+y*y) ;
            break;
          case 1:
            sum2 = sum2 + x*exp(-x*x/2)*(1-x*x/2)/(x*x+y*y);
            break ;
          case 2:
            sum2 = sum2 + x*exp(-x*x/2)*pow((1-x*x/2),2)/(x*x+y*y) ;
            break ;
          case 3 :
            sum2 = sum2+ x*exp(-x*x/2)*(1-x*x/2)*BESJ0 (b*x)/(x*x+y*y);
            break ;
           }

        x = x+del2 ;
      }

   return sum2*del2 ;
}


//-------------------------------------------------------------

double  c(double z, double kza, double t, double Qza , double d)
{
 double g = cos(z*d/2)+2*t*sin(z*d/2)/z ;
 double cn = 1+4*exp(-t*d)*cos(Qza/2)*(g*cos(kza+z*d/2+Qza/2)-(1+t*d)*cos(kza+Qza/2));
 return cn ;
}

double BESJ0(double x)
{
 double sum;
 sum= sin(x)/x;
 return sum ;
}
```

Appendix B Self-Consistent Solution to the SDW Gap Equation for the Double Well Superlattice

```
#include "stdafx.h"
#include"stdio.h"
#include"math.h"
#include <vector>
using namespace std ;
const double pi = 3.14159265 ;

struct Z{
    double z ;
    double theta;
    Z(double z,double theta)
    {
        this->z = z ;
        this->theta = theta ;
    }
} ;

double v(int k,double kza,double t, double a, double b, vector<Z>& arr_z );
double w(int k,double y);
double vv(int k, double lQy, double kza, double a, double b,double x1);
double  c(int k, double z,double kza,double t,double Qz ,double a, double b);
double BESJ0(double x) ;

void main( )
{
    double t, a, b, kza, delta, eps, deps;
    double d0, v0, v1, v2, g;

    //-----------------------------------------------------------------

    double step1  ;
    double theta ;
    //  hbo is hbar omega, e0 is epsilon_0, e1 and e2 are the
    //  quasiparticle energies; et is the sum of eps1 and eps2
    int i, j, l, nmax, nmax2, nmax4;

    //-----------------------------------------------------------------
    t =6.0;
    a = 0.2f;
    b= 1.1f;
    nmax=80;

    eps = 0.5*sqrt(pi/2.0);
    delta =0.9*sqrt(pi/2.0);

    kza= -pi;
    step1=2*pi/nmax;
    nmax4 = 5;

    double* kzaarr = new double[nmax+1];
    double* thetaarr = new double[nmax+1];
    for(j=0; j <= nmax ;j++)
    {
        kzaarr[j] = kza ;
        thetaarr[j] = pi/10 ;
        kza = kza + step1;
    }

    if(remove( "zqz3.txt" ) == -1 )
    {
        perror( "Could not delete 'ZQz3.TXT'" );
    }
    else
    {
        printf( "Deleted 'zqz3.txt'\n" );
    }
    FILE *fp4;
    if ((fp4=fopen("zqz3.txt","a+"))==NULL)
    {
        printf("cannot open this file\n");
        return    ;
    }

    fprintf(fp4,"kza    theta   e1  e2\n");
    printf("kza theta   e1  e2\n");
```

```
    //-------------------------------------------------
    //  this step initializes the file theta.txt
    //-------------------------------------------------
    for(i = 1 ; i<=nmax4 ;i++)
    {
        fprintf(fp4,"%i iterator \n" , i);
        printf("%i iterator \n" , i);
        nmax2 = -9 ;
        vector<Z> arr_z ;

        for( l = 1; l<= 2*abs(-9)+1 ;l++)
        {
            for(j=0; j <= nmax ;j++)
            {
                kza = kzaarr[j] ;
                theta=thetaarr[j] ;
                double z = 2*pi*nmax2 + kza ;
                arr_z.push_back(Z(z,theta));
            }
            nmax2 = nmax2+ 1  ;
        }
        //-------------------------------------------------------------------------------
        //  at each iteration, the program reads the current values of kza and
        //  theta; this step initializes the file z.txt
        //-------------------------------------------------------------------------------
        for(j=0; j <= nmax ;j++)
        {
            kza = kzaarr[j] ;
            d0 = eps + delta*cos(kza) ;
            v0 = v(0,kza,t,a,b,arr_z) ;
            v1 = v(1,kza,t,a,b,arr_z) ;
            v2 = v(2,kza,t,a,b,arr_z);
            deps = d0-v1-v2+v0 ;
            g = v(3,kza,t,a,b,arr_z) ;
            if(g/deps >= 0)
            {
                theta = 0.5*atan(g/deps) ;
            }
            else
            {
                theta = pi/2-0.5*atan(-g/deps);
            }
            double e2 = -v2-v1+sqrt(pow(deps ,2) + pow(g ,2)) ;
            double e1= -v0-sqrt(pow(deps ,2) + pow(g,2)) ;
            fprintf(fp4,"%f,      %f,      %f,      %f  \n", kza, theta, e1, e2);
            printf("%f  %f  %f  %f  \n", kza, theta, e1, e2);
            thetaarr[j] = theta ;
            }
    }
    fclose(fp4);
    printf( "Press RETURN to finish:" );
    char c = getchar();
}

//-------------------------------------------------------------------
double v(int k,double kza,double t, double a, double b,vector<Z>& arr_z )
{
    int  i,nmax1, nmax2 ;
    double del1  ;
    double sum1, z ;

    nmax1 = 81 ;
    nmax2 = 7*nmax1;
    del1 = 2*pi/nmax1;
    sum1 = 0.0;
    int  count = arr_z.size() ;
    for(i=0; i<count; i++)
    {
        double z = arr_z[i].z ;
        double theta = arr_z[i].theta ;

        switch(k)
        {
        case 0:
            sum1 = sum1 + c(0,z*(b-2*a)-kza,kza,t,0.0,a,b)*w(k,z-kza/(b-2*a))*pow(cos(theta),2);
            break ;
        case 1:
            sum1 = sum1 + w(k,z-(kza+pi)/(b-2*a))*c(1,z*(b-2*a)-(kza+pi),kza+pi,t,0.0,a,b) ;
            break;
        case 2:
            sum1 = sum1 + c(2,z*(b-2*a)-(kza+pi),kza+pi,t,0.0,a,b)*w(k,z-(kza+pi)/(b-2*a))*pow(sin(theta),2);
            break;
        case 3:
            sum1 = sum1 + c(3,z*(b-2*a)-kza,kza,t,pi/2,a,b)* w(k,z-kza/(b-2*a))*sin(2*theta);
            break;
        }
```

```
    }
    return sum1*del1/pi;
}


//-----------------------------------------------

double w(int k,double y)
{
    double  x, b ;
    int nmax ;
    double sum2, del2 ;
    b = 1.2f ;
    //  b=1.2 is the value of Q_yl which realizes the instability in 2D.
    sum2 = 0.0 ;
    nmax = 500 ;
    del2 = 50.0/nmax ;
    x = del2/2 ;
    for(int j = 0; j < nmax + 1 ; j++)
    {
        switch(k)
        {
        case 0:
            sum2 = sum2 + x*exp(-x*x/2)/(x*x+y*y);
            break;
        case 1:
            sum2 = sum2 + x*exp(-x*x/2)*(1-x*x/2)/(x*x+y*y);
            break ;
        case 2:
            sum2 = sum2 + x*exp(-x*x/2)*pow((1-x*x/2),2)/(x*x+y*y) ;
            break ;
        case 3 :
            sum2 = sum2+ x*exp(-x*x/2)*(1-x*x/2)*BESJ0 (b*x)/(x*x+y*y);
            break ;
        }
        x = x+del2 ;
    }
    return sum2*del2 ;
}

//-----------------------------------------------------------------
double  c(int k, double z,double kza,double t,double Qz ,double a, double b)
{
    double g1 = cos(z*(b/2-a))+2*t*sin(z*(b/2-a))/z ;
    double g2 = cos(z*a)+2*t*sin(z*a)/z ;
    double cn;

      switch(k)
        {
        case 0:
            cn=1+2*cos(z*a)*exp(-t*a)*g2+2*cos(z*a)*cos((kza+z/2)*b)*exp(-t*(b-2*a))*g1;
            break;
        case 1:
            cn = 1+2*sin(z*a)*exp(-t*(b-2*a))*g1*sin((kza+z/2)*b);
            break ;
        case 2:
            cn=1-2*cos(z*a)*exp(-t*a)*g2-2*cos(z*a)*cos((kza+z/2)*b)*exp(-t*(b-2*a))*g1;
            break ;
        case 3 :
            cn = 1+2*sin(z*a)*exp(-t*(b-2*a))*g1*cos(Qz*b/2)*sin((kza+z/2+Qz/2)*b);
            break ;
        }
    return cn ;
}

double BESJ0(double x)
{
    double sum;
    sum= sin(x)/x;
    return sum ;
}
```

Bibliography

[1] A. W. Overhauser. *Phys. Rev. Lett.*, **3**:414–416, 1959.

[2] A. W. Overhauser and A. Arrott. *Phys. Rev. Lett.*, **4**:226–227, 1960.

[3] A. W. Overhauser. *Phys. Rev. Lett.*, **3**:414–416, 1959.

[4] A. W. Overhauser. *Phys. Rev. Lett.*, **4**:462–465, 1960.

[5] A. W. Overhauser. *Phys. Rev.*, **1**67:691–698, 1968.

[6] Gabriele F. Giuliani and Giovanni Vignale. *Quantum Fermi Liquids*. Cambridge University Press.

[7] D. C. Tsui, H. L. Stormer, and A. C. Gossard. *Phys. Rev. Lett.*, **4**8(22):1559–1562, 1982.

[8] A. Pinczuk, B. S. Dennis, D. Heiman, C. Kallin, L. Brey, C. Tejedor, S. Schmitt-Rink, L. N. Pfeiffer, and K. W. West. *Phys. Rev. Lett.*, **6**8:3623–3626, 1992.

[9] Song He, S. Das Sarma, and X. C. Xie. *Phys. Rev. B*, **4**7:4394–4412, Feb 1993.

[10] B. I. Halperin, Patrick A. Lee, and Nicholas Read. *Phys. Rev. B*, **4**7:7312–7343, 1993.

[11] Gabriele F. Giuliani and J. J. Quinn. *Phys. Rev. B*, **3**1:6228–6232, 1985.

[12] J. P. Eisenstein, T. J. Gramila, L. N. Pfeiffer, and K. W. West. *Phys. Rev. B*, **4**4:6511–6514, 1991.

[13] R. J. Radtke, P. I. Tamborenea, and S. Das Sarma. *Phys. Rev. B*, **5**4:13832–13858, 1996.

[14] G. S. Boebinger, H. W. Jiang, L. N. Pfeiffer, and K. W. West. *Phys. Rev. Lett.*, **6**4:1793–1796, 1990.

[15] L. Brey, E. Demler, and S. Das Sarma. *Phys. Rev. Lett.*, **8**3:168–171, 1999.

[16] S. Das Sarma and P. I. Tamborenea. *Phys. Rev. Lett.*, **7**3:1971–1974, 1994.

[17] L. Esaki and R. Tsu. *IBM J. Res. Dev.*, **1**4:61, 1970.

[18] T. D. Golding, S. K. Greene, M. Pepper, J. H. Dinan, A. G. Cullis, G. M. Williams, and C. R. Whitehouse. *Semicond. Sci. Technol.*, **4**:311, 1990.

[19] T. Ashley, A. B. Dean, C. T. Elliot, G. J. Pryce, A. D. Johnson, and H. Willis. *Appl. Phys. Lett.*, **6**6:481, 1995.

[20] J. Hermans, D. L. Partin, C. M. Thrush, and L. Green. *Semicond. Sci. Technol.*, **8**:424.

[21] F. Bloch. *Z.Phys.*, **5**7:549, 1929.

[22] A. W. Overhauser. *Phys. Rev.*, **1**28:1437–1452, 1962.

[23] Gabriele F. Giuliani and J. J. Quinn, 1986.

[24] C. Kallin and B. I. Halperin. *Phys. Rev. B*, **3**1:3635–3647, 1985.

[25] J. J. Davies, D. Wolverson, I. J. Griffin, O. Z. Karimov, C. L. Orange, D. Hommel, and M. Behringer. *Phys. Rev. B*, **6**2:10329–10334, 2000.

[26] M. J. Snelling, E. Blackwood, C. J. McDonagh, R. T. Harley, and C. T. B. Foxon. *Phys. Rev. B*, **4**5:3922–3925, 1992.

[27] V. T. Dolgopolov, A. A. Shashkin, A. V. Aristov, D. Schmerek, W. Hansen, J. P. Kotthaus, and M. Holland. *Phys. Rev. Lett.*, **7**9:729–732, 1997.

[28] J. F. JANAK. *Phys. Rev.*, **1**78:1416–1418, 1969.

[29] A. P. Smith, A. H. MacDonald, and G. Gumbs. *Phys. Rev. B*, **4**5:8829–8832, 1992.

[30] R. J. Nicholas, R. J. Haug, K. v. Klitzing, and G. Weimann. *Phys. Rev. B*, **3**7:1294–1302, 1988.

[31] T. Ando and Y. Uemura. *J. Phys. Soc. Jpn*, **3**7:1044, 1974.

[32] A. B. Van'kov, L. V. Kulik, I. V. Kukushkin, V. E. Kirpichev, S. Dickmann, V. M. Zhilin, J. H. Smet, K. von Klitzing, and W. Wegscheider. *Physical Review Letters*, **9**7:246801, 2006.

[33] D. C. Marinescu, J. J. Quinn, and Gabriele F. Giuliani. *Phys. Rev. B*, **6**1:7245–7248, 2000.

[34] Lian Zheng, R. J. Radtke, and S. Das Sarma. *Phys. Rev. Lett.*, **7**8:2453–2456, 1997.

[35] S. Das Sarma, Subir Sachdev, and Lian Zheng. *Phys. Rev. B*, **5**8:4672–4693, 1998.

[36] J. Kolorenč, L. Smrčka, and P. Středa. *Phys. Rev. B*, **6**6:085301, 2002.